

**Frequency Modulated Continuous Wave
Radar System at ISM Band
for Short Range Indoor Positioning**

A Thesis

Presented to

the Faculty of the School of Engineering and Applied Science

University of Virginia

In Partial Fulfillment

of the Requirements for the Degree

Master of Science in Electrical Engineering

By

Yuxin Wang

Abstract

Frequency modulated continuous wave (FMCW) radar is a technique for obtaining range information from a radar by frequency modulating a continuous signal. The frequency range of FMCW radar varies from 900 MHz to 80 GHz, and one of the applications is human positioning for indoor healthcare scenarios and intelligent housing system. FMCW radar system is becoming more portable, more precise and cheaper. In this thesis, a FMCW radar system at 2.4 GHz ISM band is proposed for intelligent housing system.

The thesis proposes an economic and efficient DDS-based PLL frequency synthesizer. It can generate a frequency modulated continuous wave from 2.4 GHz to 2.5 GHz in 1 ms. The thesis uses the ADF4158 phase locked loop (PLL) chip to implement triangle frequency modulation in order to generate the 2.4 GHz continuous wave signal, and in this frequency synthesizer system, a direct digital synthesizer (DDS) chip is used, as the reference frequency of PLL, to analyze crystal-based PLL and DDS based PLL. The PLL frequency synthesizer shows high accuracy and low phase noise, and it is easy to be controlled by PC.

The FMCW radar system adopts a homodyne transceiver architecture. The thesis shows effective design of each part of the homodyne receiver, including amplifiers, filters and a mixer. The whole transceiver shows the performance in position estimation and tracking objects within 10 meters with less than 2% error.

Contents

1	Introduction	1
1.1	Research Background	1
1.2	Research Status of FMCW Radar	3
1.3	Research Status of PLL Frequency Synthesizer	5
1.4	Thesis Outline	6
2	FMCW Radar Theory	7
2.1	Working Principle of FMCW radar	7
2.2	Radar Transceiver Architecture	12
2.3	Summary	15
3	DDS-based PLL Frequency Synthesizer	16
3.1	Working Principle of Direct Digital Synthesizer	16
3.2	Phase-locked Loop Frequency Synthesizer	22
3.2.1	Working Principle of PLL Synthesizer	23
3.2.2	Phase Noise Analysis	25
3.3	DDS-based PLL Synthesis Technology	29
3.4	Summary	31
4	FMCW Radar System Design and Test	32
4.1	Radar System Design	33
4.1.1	LNA Design and Test	33
4.1.2	Filter Design	34
4.1.3	Mixer	35

4.1.4 Power Amplifier Text.....	36
4.1.5 Radar Components Summary.....	36
4.2 Human Indoor Positioning and Tracking.....	37
4.3 Analysis and Future Work.....	41
Appendix	48
Bibliography	53

Chapter 1

Introduction

The word “radar” is an acronym derived from the phrase RADIO Detection And Ranging and it is applied for detecting and tracking objects at certain distances. The basic principle of radar is simple – signals traveling at the speed of light are transmitted, reflected off a target and then returned as an echo.

1.1 Research Background

The history of radar dated back to experiments by Heinrich Hertz in 1886 that showed that radio waves were reflected by metallic objects, and in 1900 Tesla described a concept for electromagnetic detection and velocity measurement in an interview, [1]. In 1903 and 1904 , the German engineer Hülsmeyer experimented with ship detection by radio wave reflection, an idea advocated again by Marconi in 1922. In that same year, Taylor and Young of the U.S. Naval Research Laboratory (NRL) demonstrated ship detection by radar and in 1930 Hyland, also of NRL, first detected aircraft (albeit accidentally) by radar, setting off a more substantial investigation that led to a U.S. patent for what would now be called a continuous wave (CW) radar in 1934.

Early radar development was driven by military necessity, including surveillance, navigation, and weapons guidance for ground, sea, air, and space vehicles. And now, radar enjoys an increasing range of applications, [2]. One of the most common is the police traffic radar used for enforcing speed limits. Another is the “weather radar” familiar to every viewer of local television news. Another radar application is found in the air traffic control systems used to guide commercial aircraft. Finally, satellite and airborne radar is an important tool in mapping earth topology and environmental characteristics such as water and ice conditions, forestry conditions, land usage. While

this sketch of radar applications is far from exhaustive, it does indicate the breadth of applications of this remarkable technology.

Radar can be classified as primary radar and secondary radar, which is shown in figure 1.1: a primary radar transmits signals with high frequency toward the targets. The transmitted signals are reflected by the target and then received by the same radar. And secondary radar works with active answer signals.

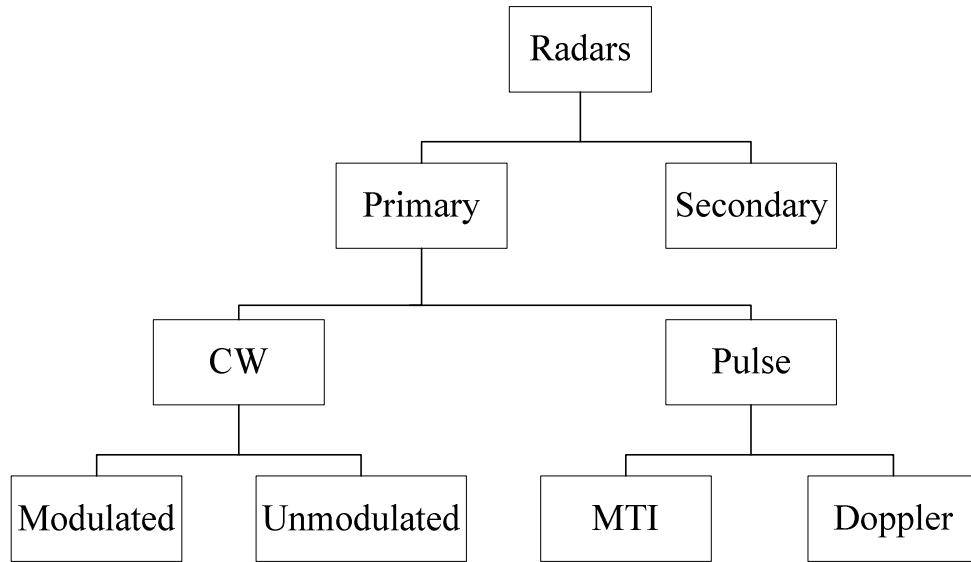


Figure 1.1 Simplified classification of radar

CW radars continuously transmit a high-frequency signal and the reflected signal is also received and processed continuously. The transmitted signal of unmodulated radar is constant in amplitude and frequency. Transmitting unmodulated power of CW radar can only measure the speed using the Doppler effect, but it cannot measure a range and cannot differ between two reflecting objects. This is achieved in modulated CW radars using the frequency shifting method. In this method, a signal changing in frequency constantly around a fixed reference is used to detect objects. Pulsed radar transmits high power, high-frequency pulses toward the target, then it waits for the echo of the transmitted signal before it transmits a new pulse.

Each method has its advantages over the other. The advantages of pulsed radar include increased range, lower power consumption, and it does not rely on the Doppler Effect to determine movement. Continuous wave radar benefits include a continuous updating of target, higher resolution, and doesn't have the minimum target distance.

1.2 Research Status of FMCW radar

As the name suggests, frequency modulated continuous wave (FMCW) radar is a technique for obtaining range information from a radar by frequency modulating a continuous signal. The technique has a very long history, but in the past its use has been limited to certain applications, such as radio altimeters. However, there is now renewed interest in the technique for three main reasons, [3]. First, the most general advantage possessed by FMCW radar is that the modulation is readily compatible with a wide variety of solid-state transmitters. Second, the frequency measurement which must be performed to obtain range measurement from such a system can now be performed digitally, for example, using a processor based on the fast Fourier transform (FFT).

Benefits of FMCW over other modulated CW waveforms are: 1) the ability to control the range and to obtain very efficient use of the spectrum; 2) the ease with which the range resolution can be changed, and the way in which very high range resolutions can be obtained without requiring wide IF and video bandwidths.

During the second world war, FMCW radar was used for bomb aiming radars and in 1946 an FMCW surveillance radar was built. This obtained its modulation by “pushing” a magnetron. It did not work very well, and the reason for building it is unclear.

Bamck [4] first discussed the application of moving target indication (MTI) type processing to FMCW radar. In the meantime, Fuller may have been the first to apply FMCW to automotive radar, but in this case the modulation was almost a “side effect” of the use of frequency scanning to scan the beam.

A major step forward was made in the mid 1970's when digital signal processing became available to perform the signal processing to extract the range information from the received signals. Before digital processing became available, many earlier FMCW radars, such as those discussed above, used single band-pass filters to detect signals at a single range, and varied the sweep rate systematically to search all the possible range gates, [5]. This makes very inefficient use of the radar's observation times. On the other hand, FMCW radio altimeters have long used a closed-loop system to adjust the sweep period to keep the beat frequency from the ground within a single range bin. Since only a single range-gate is required, this approach achieves efficient use of the energy without needing to process many range gates. Modern radio altimeters, however, do

also use digital (FFT-based) processing as well as this technique. It is now commonplace to use a FFT, or other digital frequency analysis techniques, to analyze the mixture of beat frequencies corresponding to the targets at different ranges.

In 1998, McClanahan and other researchers in United States developed a ranging system based on pulsed radars, of which the center frequency was 3.2 GHz, the error of test data was less than 10%. In 1999, Li developed a FMCW radar obtaining range and angle information of obstacles. Its working frequency was 77 GHz, transmitting signal linearity was better than 0.5%, maximum range was 100 m, range resolution was less than 1m. It had a wide application for vehicle collision avoidance system because of the simple structure.

In 1999, William H. Haydl developed a FMCW radar integrated on a 0.88 mm^2 single chip. Its working frequency is 94 GHz, DC input power is 0.7 W, RF power is 10 mW. The receiver had 6 dB noise figure and 10 dB gain. The whole front end included VCO, PA, LNA, mixer and coupler. In 2003, Musch used N-fractional PLL to develop a FMCW radar. The system has high linearity and measurement error was about 0.8 mm, [6].

In 2016, Gitae Pyo [7] and his team developed a CMOS transceiver IC for a single-antenna FMCW radar at K band. The transceiver achieved the output power of -1.6 dBm , phase noise of -105 dBc/Hz at 1 MHz offset, receiver gain of 15.3 dB, and the noise figure of 11.6 dB. including a $1.7 \text{ mm} \times 0.9 \text{ mm}$ pad.

Nowadays, FMCW radar is widely used in various fields from civil to military applications. It can be used for imaging purposes. Automotive FMCW radar can be used to record velocity violations on roads. It can also be used as driver intelligence systems to improve driving conditions and avoid collisions. It can be also employed for ship navigation and identification. FMCW radars can also be used target detection under the ground clutter environment, [8]. Some authors presented FMCW radars for geosciences to measure wind speed and directions.

On the other hand, it is frequently used for indoor human tracking for indoor healthcare scenarios, such as fall detection of elderly people or breath detection, and intelligent housing system. FMCW radar for indoor human tracking is becoming more portable, more precise and cheaper. In this work, a FMCW radar system at 2.4 GHz is proposed for intelligent housing systems.

1.3 Research Status of PLL Frequency Synthesizer

The phase locked loop is a control system that can generate an output signal whose phase is related to the phase of an input signal. While there are several differing types, it is easy to initially visualize as an electronic circuit consisting of a variable frequency oscillator and a phase detector. The oscillator generates a periodic signal, and the phase detector compares the phase of that signal with the phase of the reference signal, adjusting the oscillator to keep the phases matched, [9]. Bringing the output signal back toward the input signal for comparison is called a feedback loop since the output is "fed back" toward the input forming a loop.

PLLs date back to the 1920s, but their popularity and applications took off with the introduction of the monolithic PLL, [10]. The 4046 CMOS Micropower PLL, which RCA introduced in the 1970s, is one of the early PLL ICs. These ICs found use in many applications, including frequency synthesis, FM demodulation and modulation, voltage-to-frequency conversion, and data synchronization. The 4046 integrated two types of phase detectors—a linear mixer and an edge-triggered phase/frequency detector—with a VCO (voltage-controlled oscillator) and an output buffer that allowed designers to use the tuning voltage for demodulation applications.

The most common type of PLL for SOC (system-on-chip) applications is the frequency-multiplying PLL. This type of PLL generates a high-frequency clock from a low-frequency crystal or another reference. Applications for frequency-multiplying PLL are widespread and include logic clocking and RF local-oscillator synthesis. Figure 1.2 shows the history and development of radar and PLL.

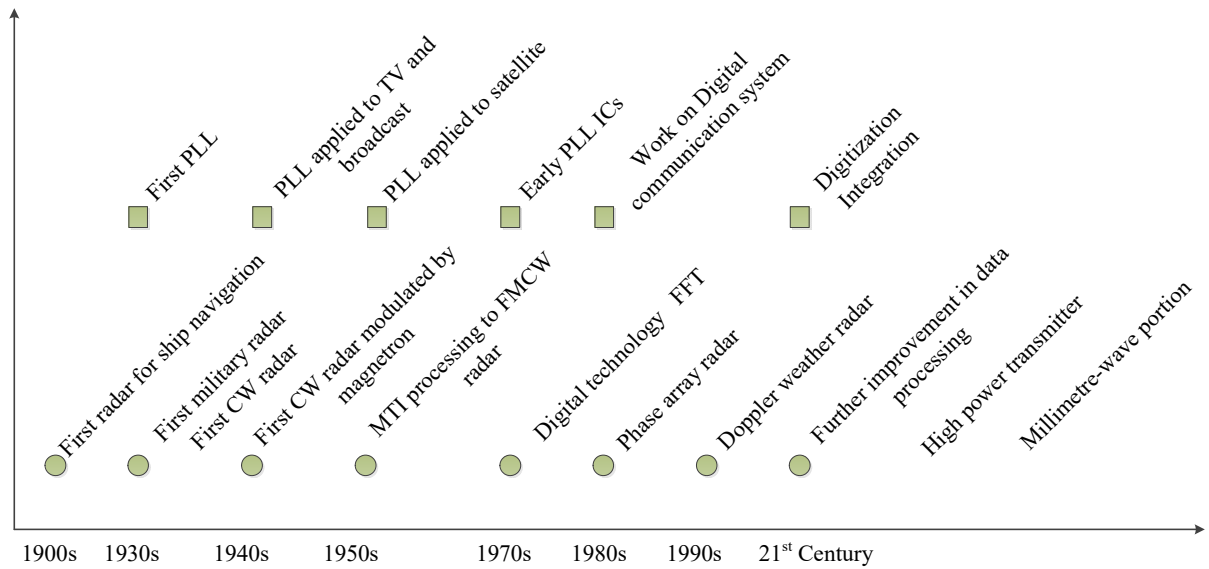


Figure 1.2 History of the development of radar and PLL

1.4 Thesis Outline

This thesis proposes a FMCW radar at ISM band for indoor human positioning and tracking, including research about DDS-based PLL frequency synthesizer and homodyne receiver architecture. The content of this thesis is organized as follows:

In Chapter 2, the thesis presents the working principle and equations of FMCW radar, and parameters of the indoor FMCW radar, including range and velocity information, are given. Then in Microwave Office, the whole radar system is simulated.

In Chapter 3, the thesis designs the frequency synthesizer for the FMCW radar. The PLL frequency synthesizer is based on a DDS board. In this chapter, the thesis discusses the working principle of DDS and PLL, and gives the measurement and analysis of power spectrum and phase noise of the DDS-based PLL board.

In Chapter 4, the thesis discusses the design of FMCW radar transmitter and homodyne receiver. Test and analysis of each component is given. And the thesis does test and analysis of the whole FMCW radar system. It shows that the whole transceiver has a good performance to position and track objects in 10 meter with 2% error.

Chapter 2

FMCW Radar Theory

In the past decade, portable radar systems have experienced tremendous growth. Such rapid growth has created demand for portable wireless devices that are smaller, lighter, cheaper and of higher performance than ever, and this drives IC designers and engineers to innovate new system architectures and circuit topologies. In this work, we choose frequency modulated continuous wave (FMCW) radar to implement indoor positioning. FMCW radar, it is a type of radar system where a stable frequency continuous-wave radio energy is transmitted and then received from reflecting objects. This work adopts a homodyne architecture in FMCW radar receiver.

2.1 Working Principle of FMCW radar

As described above, FMCW radar is a special type of radar sensor which radiates continuous transmission power like a simple continuous wave radar. In contrast to normal CW radar, FMCW radar can change its operating frequency during the measurement: that is, the transmission signal is modulated in frequency (or in phase).

Simple continuous wave radar devices without frequency modulation have the disadvantages [11] that they cannot determine target range because they lack the timing mark necessary to allow the system to time accurately the transmit and receive cycle and to convert this into range. Such a time reference for measuring the distances of stationary objects, but can be generated using frequency modulation of the transmitted signal. In this method, a signal is transmitted, which increases or decreases in the frequency periodically. When an echo signal is received, that change of frequency gets a delay Δt similar to the pulse radar technique. In pulse radar, however, the runtime must be measured directly. For a FMCW radar, the distance measurement is accomplished by comparing the frequency of the received signal to a reference, which is usually the transmission signal. And the duration of the transmission signal is

substantially greater than the required receiving time for the installed distance measuring range.

There are several modulation patterns used for different measurement purposes: sawtooth modulation, triangular modulation, square-wave modulation (simple frequency-shift keying, FSK) and stepped modulation (staircase voltage). Sawtooth modulation is used in a large range combined with a negligible influence of Doppler frequency. And for square-wave modulation, it is used for a very precise distance measurement at close range by phase comparison of the two echo signal frequencies. But the disadvantage is that the echo signals from several targets cannot be separated from each other, and that this process enables only a small unambiguous measuring range.

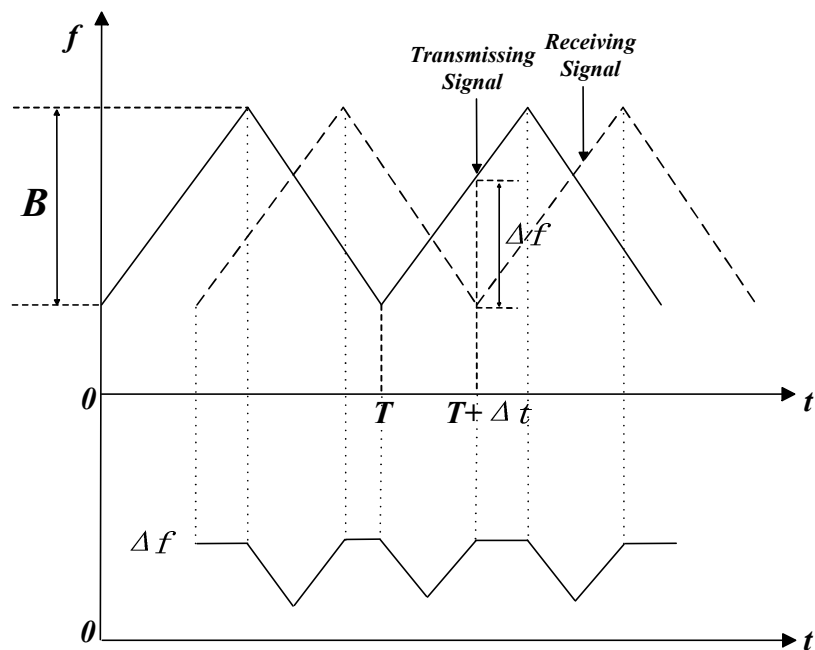


Figure 2.1 Working principle of FMCW radar for stationary targets

In this thesis, triangular modulation is issued, the carrier signal of the radar is frequency-modulated by triangular waves. The radar transmits and receives signals with a frequency deviation, as shown in figure 2.1. The frequency difference is proportional to the time difference between the transmitted and received signals, which in turn is proportional to the distance between the transmitter and target.

Assuming that the transmitter frequency increases linearly with time and that there is a reflecting object at a distance, the time varying amplitude, frequency and phase is shown below:

$$u_s = A_s \cos \varphi_s(t) \quad (2.1)$$

$$f_s(t) = f_c + \frac{2B}{T}t \quad (2.2)$$

$$\phi_s(t) = 2\pi \int_0^t f_s(t)dt + \varphi_{so} = 2\pi(f_c t + \frac{B}{T}t^2) + \varphi_{so} \quad (2.3)$$

where A_s is the signal amplitude, f_c is the carrier frequency, φ_{so} is the initial phase. B is the sweep rate in Hz. An echo signal will return after the transit time Δt , and the phase of the received signal can be expressed as:

$$\varphi_E(t) = \varphi_s(t - \Delta t) = 2\pi(f_c(t - \Delta t) + \frac{B}{T}(t - \Delta t)^2) + \varphi_{so} \quad (2.4)$$

The beat frequency component can be written as:

$$\begin{aligned} u_d(t) &= U_D \cos(\varphi_s(t) - \varphi_E(t)) \\ &= U_D \cos \left[2\pi \left(\frac{2B}{T}t\Delta t + f_c\Delta t - \frac{B}{T}\Delta t^2 \right) \right] \end{aligned} \quad (2.5)$$

where U_D is the amplitude of the beat note signal. If there is no Doppler frequency shift, the beat frequency is a measure of the target's range:

$$\Delta t = \frac{2r_o}{c_0} \quad (2.6)$$

According to triangle relationship:

$$\frac{\Delta t}{\Delta f} = \frac{T/2}{B} \quad (2.7)$$

From equation (2.6) and (2.7), the distance from target can be expressed as:

$$R = \frac{c_0 T}{4B} \Delta f \quad (2.8)$$

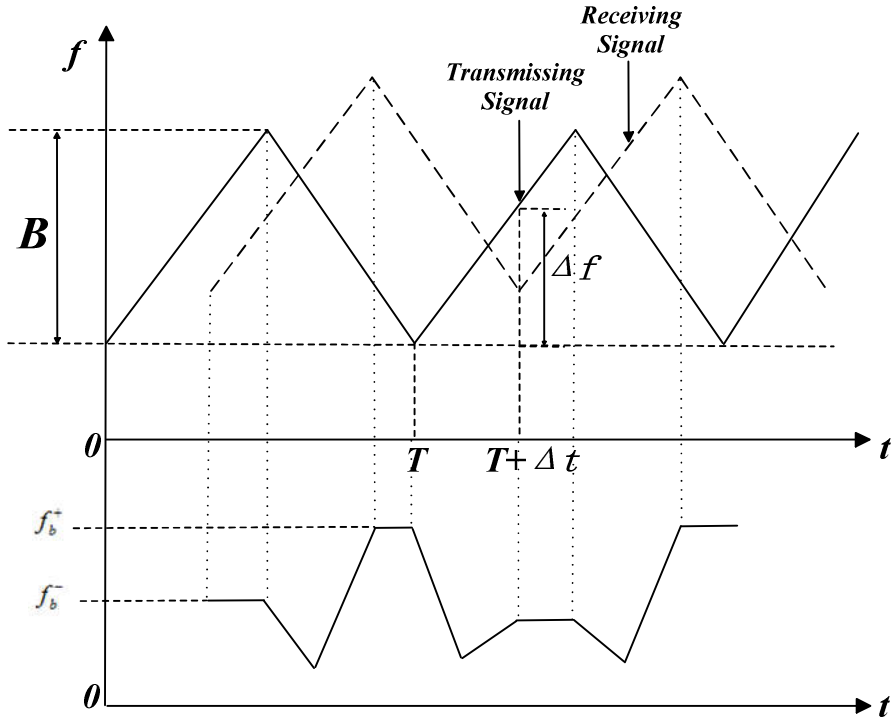


Figure 2.2 Working principle of FMCW radar for moving targets

For a moving object [13], as figure 2.2 illustrates, the frequency of received waves is shifted because of time delay and Doppler shift, which results in two different beat frequencies. Denoting the modulation range and start frequency as B and f_o , the frequency of transmitting signal is shown below:

$$f_t^+(t) = f_o + kt \quad 0 \leq t < T/2 \quad (2.9)$$

$$f_t^-(t) = f_o + 2B - kt \quad T/2 \leq t < T \quad (2.10)$$

of which the instantaneous phase is

$$\phi_t^+(t) = 2\pi \int_0^t f_t^+ dt + \theta_o = 2\pi f_o t + \pi k t^2 + \theta_o \quad 0 \leq t < T/2 \quad (2.11)$$

$$\phi_t^-(t) = 2\pi \int_0^t f_t^- dt + \theta_o = 2\pi(f_o + 2B)_o(t - T/2) - \pi k(t^2 - T^2/4) + \phi_t^+(T/2) \quad T/2 \leq t < T \quad (2.12)$$

Thus, the instantaneous phase of echo signal can be expressed as:

$$\phi_r^+(t) = 2\pi f_o(t - \tau(t)) + \pi k(t - \tau(t))^2 + \theta_o \quad \tau \leq t < T/2 + \tau \quad (2.13)$$

$$\phi_r^-(t) = 2\pi(f_o + 2B)_o(t - \tau(t) - T/2) - \pi k[(t - \tau(t))^2 - T^2/4] + \phi_t^+(T/2) \quad T/2 + \tau \leq t < T \quad (2.14)$$

When $\phi_b^+ = \phi_t^+ - \phi_r^+$ and $\phi_b^- = \phi_t^- - \phi_r^-$, the beat frequency is obtained:

$$f_b^+(t) = \frac{1}{2\pi} \frac{d\phi_b^+}{dt} = k\tau(t) - f_d \quad \tau \leq t < T/2 \quad (2.15)$$

$$f_b^-(t) = \frac{1}{2\pi} \frac{d\phi_b^-}{dt} = k\tau(t) + f_d \quad T/2 + \tau \leq t < T \quad (2.16)$$

Since T is much greater than τ :

$$f_b^+(t) = k\tau(t) - f_d \quad \tau \leq t < T/2 \quad (2.17)$$

$$f_b^-(t) = k\tau(t) + f_d \quad T/2 \leq t < T \quad (2.18)$$

where $f_d = f_{delay} + f_{doppler} = \frac{t_d \times B}{T/2} + \frac{2f_c \times v_r}{c}$, $t_d = \frac{2r_o}{c}$

As long as we can get the value of two beat frequency $f_b^+(t)$ and $f_b^-(t)$, we can get the value of distance and velocity:

$$r_o = \frac{c_o T}{4B} \left(\frac{f_b^+ + f_b^-}{2} \right) \quad v_r = \frac{c_o}{2f_c} \left(\frac{f_b^+ - f_b^-}{2} \right) \quad (2.19)$$

$$r_o = \frac{c_o T}{4B} \left(\frac{f_b^+ + f_b^-}{2} \right) \quad v_r = \frac{c_o}{2f_c} \left(\frac{f_b^+ - f_b^-}{2} \right)$$

The frequency range of ISM band is from 2.4 GHz to 2.5 GHz, the maximum bandwidth B is 100 MHz. Since this FMCW radar is used inside building, the detectable distance doesn't need to be very large. In this work, we assume R_{\max} is 30 m, it's easy to get delay time for maximum range:

$$t_d = \frac{2R_{\max}}{c_o} = 0.2 \mu s \quad (2.20)$$

The modulation period should be larger than the delay time for the maximum range. According to papers [31]-[36], most modulation periods of FMCW radar at 2.4 GHz are from 1ms to 10ms. In this thesis, we use ADF4158 PLL synthesizer as frequency source. In ADF4158 chip, the minimum modulation period for 2.4-2.5 GHz is 0.8 ms [14]. In this system, we set the modulation period as 1 ms. According to equation (2.8), the maximum beat frequency can be determined by:

$$f_{b\max} = \frac{4BR_{\max}}{cT} = 40 kHz \quad (2.21)$$

According to formula for distance, we can get the formula for velocity resolution ideally as follows,

$$\Delta v = \frac{c_o}{2f_c} \left(\frac{f_b^+ - f_b^-}{2} \right) = \frac{c_o}{2f_c} f_d = \frac{c_o}{2f_c} \Delta f_r \quad (2.22)$$

where Δf_r is frequency resolution of receiver, which depends on the frequency resolution of spectrum analyzer or FFT sampling frequency.

For FFT, the spectrum computed from the sampled signal has a frequency resolution Δf_r . Calculate the frequency resolution with the following equation:

$$\Delta f_r = \frac{1}{T_s} = \frac{f_s}{N} \quad (2.23)$$

where T_s is the acquisition time, N is the number of samples and f_s is the sampling frequency. Thus, frequency resolution depends on how long the acquisition time is. And it is necessary to consider the acquisition time because we need to calculate distance information before the object moving. We do 25 times FFT and hope the total acquisition time should be less than 0.5s, then frequency resolution should be larger than 50 Hz. According to equation (2.22), the velocity resolution is larger than 3 m/s, it can be seen that FMCW radar is not a good method to measure human indoor walking velocity because of such high velocity resolution.

2.2 Radar Transceiver Architecture

There are three common receiver architectures: heterodyne, homodyne and image-reject, all of which have different advantages and disadvantages. When designing a RF receiver, the choice of architecture is primarily determined by criteria including complexity, cost, power dissipation and the number of external components.

In a homodyne or direct conversion receiver, the incoming RF signal is down-converted to baseband (zero frequency) in one step by mixing with an oscillator output of the same frequency. The output baseband signal is then filtered with a low-pass filter to select the desired channel. This is illustrated in the block diagram in figure 2.3.

Using a homodyne receiver architecture, the difference frequency between the transmitted signal and received signal can be easily obtained if the frequency swept transmit signal is used for the LO down conversion. Consequently, this architecture is the preferred solution.

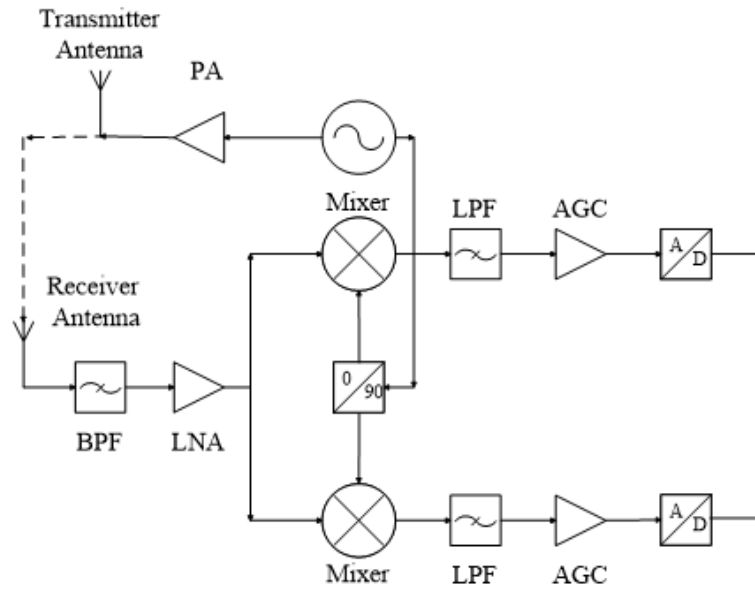


Figure 2.3 Simplified block diagram of homodyne architecture

The main advantage of a homodyne receiver [18] is that it solves the image problem because the input RF signal is down-converted directly to baseband without any IF stage. For the image problem, the homodyne receiver shown in figure 2.4 operates with double-sided signals, which overlap the positive and negative parts of the input spectrum. Consequently, the image frequency problem is circumvented because $\omega_{IF} = 0$. As a result, no image filter is required.

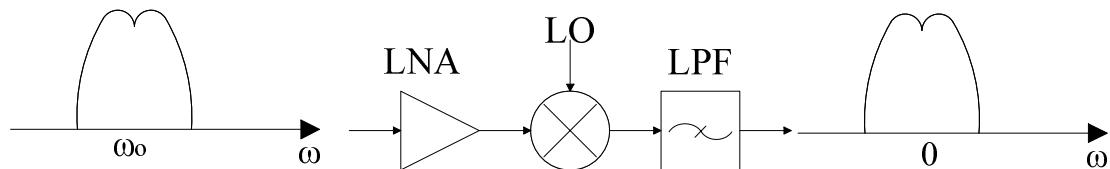


Figure 2.4 Simple homodyne receiver working principle

Another advantage is that it is easy to implement. Since it does not require any high frequency band-pass filters, which are usually implemented off-chip in a super-heterodyne receiver for appropriate selectivity, the homodyne requires less number of external components. However, the homodyne architecture does suffer DC offsets. Also, since the mixer output is a baseband signal, it can easily be corrupted by the large flicker noise of the mixer, especially when the incoming RF signal is weak.

LO leakage can result in DC offset, when the isolation between the LO port and the inputs of the mixer and the LNA is not infinite. The leakage signal appearing at the inputs of the LNA and mixer is mixed with the LO signal, which provide a DC

component at the output of the mixer. This phenomenon is called self-mixing. Another phenomenon arises if a large interferer leaks from the LNA or mixer input to the LO ports and is multiplied by itself. The principle is similar with self-mixing. And it is exacerbated if self-mixing varies with time.

Even-order nonlinearity is also a problem in homodyne down conversion systems. [19] Two strong interferers will generate a low-frequency beat. Because mixers exhibit a finite isolation from the RF input to the IF output due to asymmetry in the mixing core, the low-frequency beat will appear in the IF port. Besides, the mixer RF port may also suffer from even-order distortion, requiring special attention in the design.

Next, some basic parameters of FMCW radar system are shown below:

(1) Working Frequency: The working frequency of a transmitter and a receiver includes center frequency and bandwidth. In this thesis, the FMCW radar uses industrial, scientific and medical (ISM) radio bands, which is reserved internationally for the use of radio frequency (RF) energy for industrial, scientific and medical purposes other than telecommunications. The working frequency is from 2.4 GHz to 2.5 GHz, so the center frequency is 2.45 GHz and bandwidth is 100 MHz.

(2) Output Power: Output power is the power sent to the antenna from the last stage of the transmitter. According to the FCC rules, the transmit power limit at 2.4 GHz is 30 dBm (1 Watt), the antenna gain is 6 dBi.

(3) Noise Figure: Noise figure is the measure of degradation of the signal-to-noise ratio (SNR), caused by components in a transceiver chain. It is defined as

$$NF = \frac{SNR_{in}}{SNR_{out}}, \text{ where } SNR_{in} \text{ and } SNR_{out} \text{ are the input and output SNR}$$

respectively. If several devices are cascaded, the total noise factor can be expressed as equation (2.28), the measurement of system noise figure will be discussed in chapter 4.

$$F = F_1 + \frac{F_2 - 1}{G_1} + \frac{F_3 - 1}{G_1 G_2} + \frac{F_4 - 1}{G_1 G_2 G_3} + \dots + \frac{F_n - 1}{G_1 G_2 G_3 \dots G_{n-1}} \quad (2.28)$$

(4) Receiver Sensitivity: Sensitivity in a receiver is normally taken as the minimum input signal required to produce a specified output signal having a specified SNR and is defined as the minimum signal-to-noise ratio times the mean noise power. For a signal impinging on the antenna, sensitivity is known as minimum operational sensitivity (MOS):

$$MOS = SNR \cdot kT_o B \cdot NF / G \quad (2.29)$$

where k is Boltzmann's constant, T_o is effective noise temperature of the receiver input and G is system gain.

According to equation (2.21), the bandwidth of IF frequency is inversely proportional to modulation period. When T increases, B decreases and results in smaller receiver sensitivity. The radar equation is shown in equation (2.30). On one hand, smaller receiver sensitivity means larger detection range, and more discussion about radar equation will be shown in chapter 4. On the other hand, we need to have smaller frequency resolution for a smaller IF bandwidth, and flicker noise at low frequency will have larger effect on power spectrum.

$$R_{\max} = \sqrt[4]{\frac{P_t G_t G_r \lambda^2 \sigma}{(4\pi)^3 P_{\min}}} \quad (2.30)$$

where P_t is transmit power, G_t and G_r are transmitting and receiving antenna gain, λ is transmit wavelength, σ is target radar cross section, P_{\min} is the minimum detectable signal.

We have discussed the modeling analysis of FMCW radar, a summary of FMCW radar is shown in table 2.2:

Table 2.2 FMCW Radar Main Parameters

Radar Parameter	Value
FMCW Waveform	Triangle
Frequency Deviation (Bandwidth)	100 MHz
Frequency Band	ISM Band (2.4-2.5 GHz)
Maximum range	30 m
Modulation Period	1 ms
Maximum Beat Frequency	40 kHz
Maximum Transmitter Power	30 dBm
Band-pass Filter Range	2.4-2.5 GHz
Low-pass Filter Range	0-40 kHz
Mixer Attribute	Down Converter

2.3 Summary

After talking about the history and development of FMCW radar in chapter 1. In

chapter 2, the thesis first discusses about working principle of FMCW radar, including range formula for stationary targets and moving targets, and then the thesis gives the model of FMCW radar for indoor positioning, including maximum range, range resolution, velocity resolution and modulation period. In section 2.2, the thesis gives some introduction about three different types of receivers: heterodyne, homodyne and image-reject receivers. In this chapter, we choose the homodyne receiver to build the FMCW transceiver architecture.

Chapter 3

DDS-based PLL Frequency Synthesizer

A phase locked loop is a nonlinear feedback loop control system which is used for synchronization of the frequency and phase of a locally generated signal with that of an incoming signal. The PLL includes a voltage controlled oscillator (VCO), a phase detector, several dividers and a loop filter. On the other hand, DDS is an emerging and maturing signal generation technology, which consists of phase accumulator, lookup table and DAC converter. [20] In this thesis, we use a DDS-based PLL synthesizer as frequency source of FMCW radar transceiver. It offers very many advantages, including high levels of stability and accuracy. It is also easy to be controlled from digital circuitry such as microprocessors.

3.1 Working Principle of Direct Digital Synthesizer

As the name suggests this form of synthesis generates the waveform directly using digital techniques. This is different from the more familiar indirect synthesizers that use a phase locked loop as the basis of their operation.

A direct digital synthesizer operates by storing the points of a waveform in digital format, and then recalling them to generate the waveform. The rate at which the synthesizer completes one waveform then governs the frequency. The overall block diagram is shown below, but before looking at the detailed operation of the synthesizer it is necessary to look at the basic concept behind the system.

The operation can be envisaged more easily by looking at the way that phase progresses over the course of one cycle of the waveform, [21]. This can be envisaged as the phase progressing around a circle. As the phase advances around the circle, this corresponds to advances in the waveform.

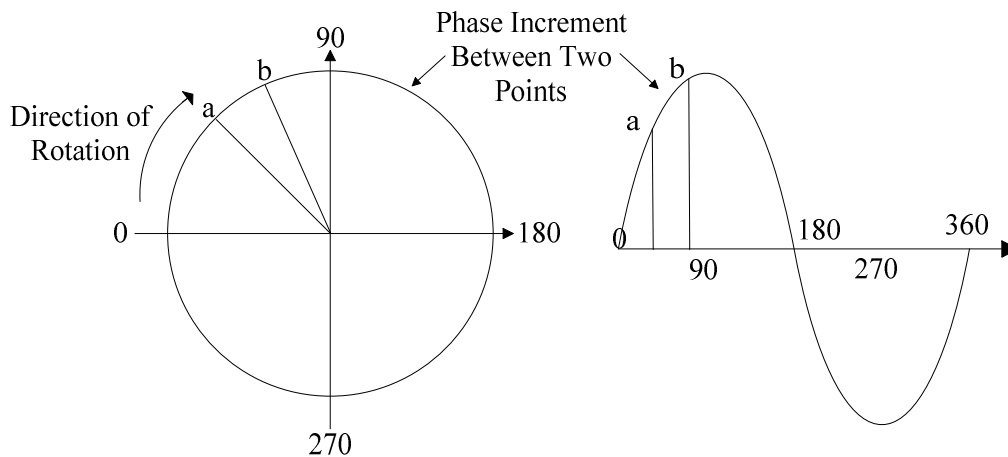


Figure 3.2 Operation of the phase accumulator in a direct digital synthesizer

Once the phase has been determined it is necessary to convert this into a digital representation of the waveform. This is accomplished using a waveform map. This is a memory which stores a number corresponding to the voltage required for each value of phase on the waveform. In the case of a synthesizer of this nature it is a sine look up table as a sine wave is required. In most cases the memory is either a read only memory (ROM) or programmable read only memory (PROM), [22]. This contains a vast number of points on the waveform, very many more than are accessed each cycle.

The next stage in the process is to convert the digital numbers coming from the sine look up table into an analogue voltage. This is achieved using a digital to analogue converter (DAC). This signal is filtered to remove any unwanted signals and amplified to give the required level as necessary.

Tuning is accomplished by increasing or decreasing the size of the step or phase increment between sample points. A larger increment at each update to the phase accumulator will mean that the phase reaches the full cycle value faster and the frequency is correspondingly high. Smaller increments to the phase accumulator value means that it takes longer to increase the full cycle value and a correspondingly low value of frequency. In this way, it is possible to control the frequency. It can also be seen that frequency changes can be made instantly by simply changing the increment value. There is no need to a settling time as in the case of phase locked loop based synthesizer.

These synthesizers do have some disadvantages, [23]. There are numbers of spurious signals which are generated by a direct digital synthesizer. The most important of these is one called an alias signal. Here images of the signal are generated on either

side of the clock frequency and its multiples. For example if the required signal had a frequency of 5 MHz and the clock was at 25 MHz then alias signals would appear at 20 MHz and 30 MHz as well as 45 MHz and 55 MHz, etc.. These can be removed by a low pass filter. Also, some low level spurious signals are produced close in to the required signal. These are normally acceptable in level, although for some applications they can cause problems. Figure 3.3 shows alias signals of AD9833 DDS chip at 5 MHz output.

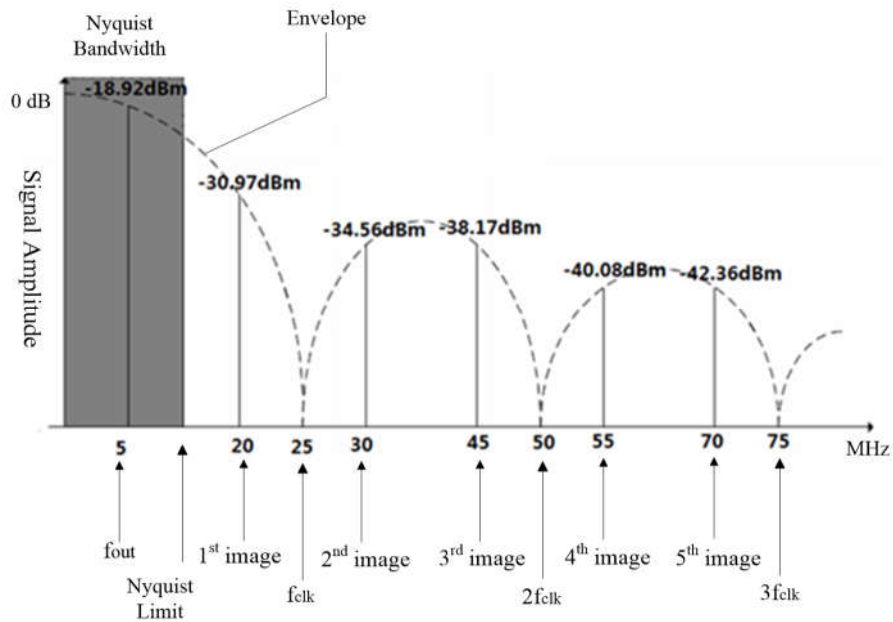


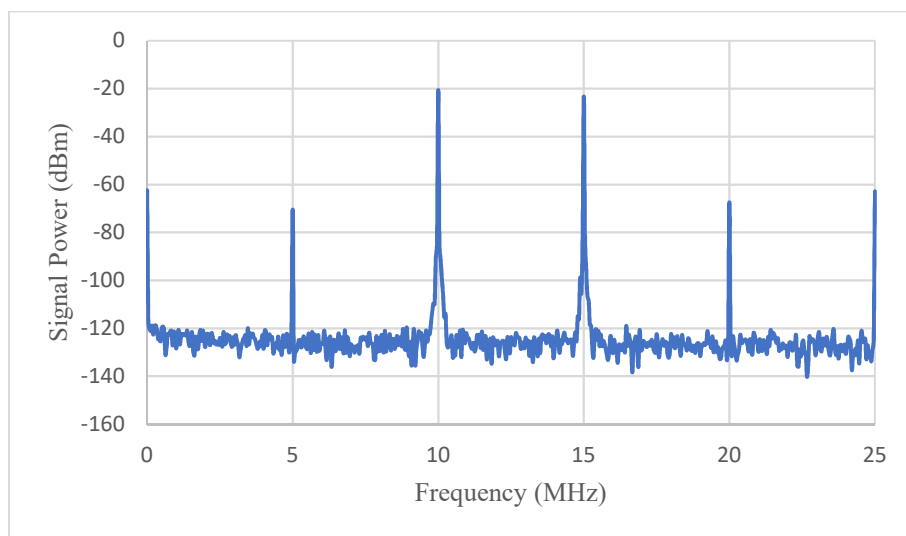
Figure 3.3 Aliasing in a DDS power spectrum

There are other “spurious” signals. Unlike a PLL-based system, the higher-order harmonics of the fundamental output frequency in a DDS system will fold back into the baseband because of aliasing. These harmonics cannot be removed by the antialiasing filter. For instance, if the clock frequency is 100 MHz, and the output frequency is 30 MHz, the second harmonic of the 30 MHz output signal appears at 60 MHz, but also at $100 - 60 = 40$ MHz (the aliased component). Similarly, the third harmonic (90 MHz) appears in band at $100 - 90 = 10$ MHz, and the fourth at $120 - 100$ MHz = 20 MHz. Higher order harmonics also fall within the Nyquist bandwidth.

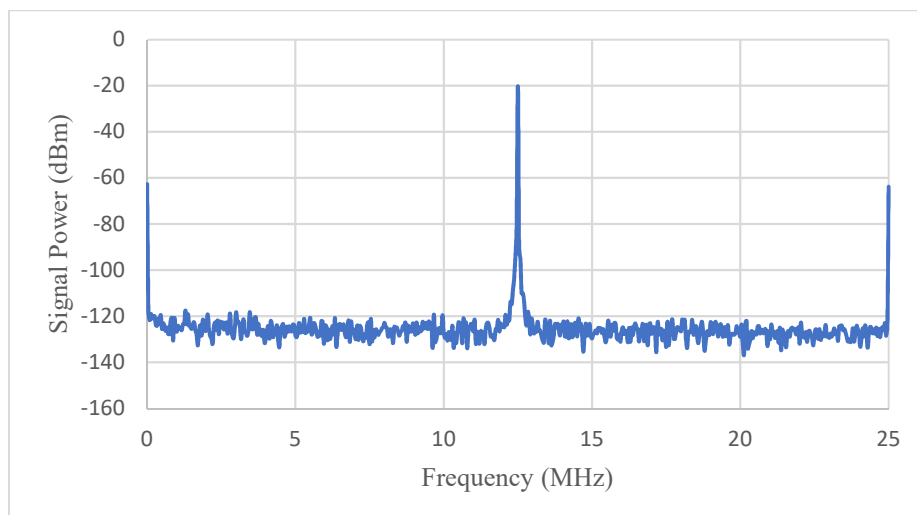
Another source of spurs [25] is switching transients that arise within the internal physical architecture of the DAC. Non-symmetrical rising and falling switching characteristics such as unequal rise and fall time will also contribute to harmonic distortion. The amount of distortion is determined by the effective ac or dynamic transfer function. Transients can cause ringing on the rising and/or falling edges of the

DAC output waveform. Ringing tends to occur at the natural resonant frequency of the circuit involved and may show up as spurs in the output spectrum.

In this thesis, we use the AD9833 board to generate reference frequency of PLL. This board is a low power, programmable waveform generator. The output frequency and phase are software programmable, allowing easy tuning. No external components are needed. The frequency registers are 28 bits wide. With a 25 MHz clock rate, resolution of 0.1 Hz can be achieved. Figure 3.4 shows power spectra at different output, it can be seen that alias signals and spurs decrease with the increase of output frequency. In the DDS-based PLL frequency synthesizer, shown in figure 3.4(b), we choose 12.5 MHz (Nyquist Limit) as DDS output frequency.



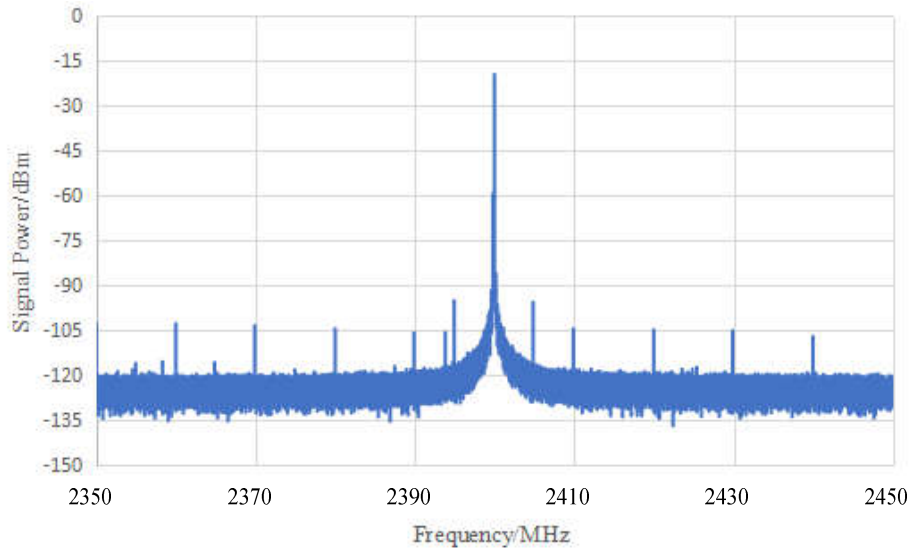
(a) $f_{out}=10$ MHz



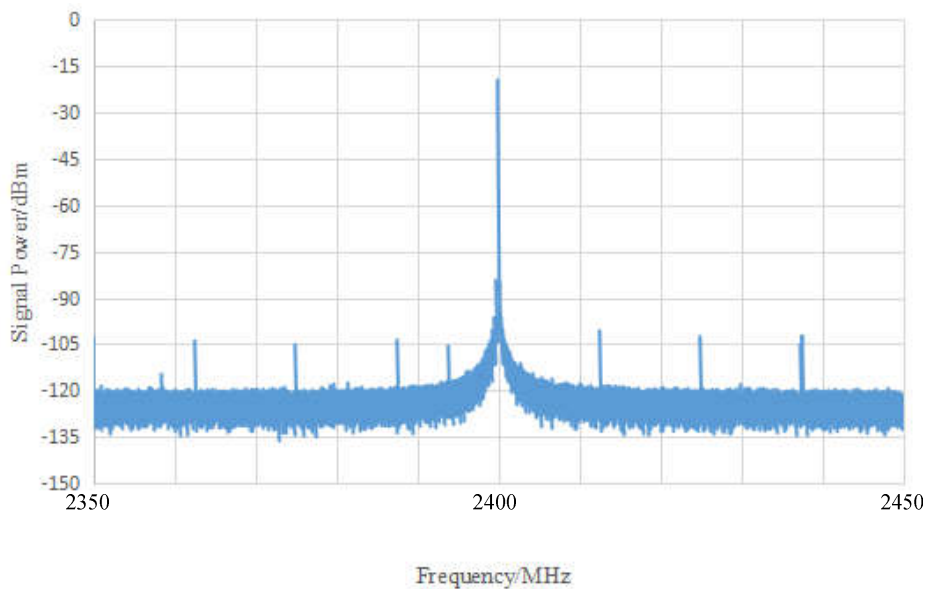
(b) $f_{out}=12.5$ MHz

Figure 3.4 DDS power spectrum

Since we use DDS signal as the reference frequency of PLL, quality of DDS power spectrum can influence output frequency of PLL. Figure 3.5 shows the PLL output power spectrum when $f_{DDS}=10$ MHz and $f_{DDS}=12.5$ MHz. It is easy to find that the smaller spurs the DDS power spectrum has, the better the PLL power spectrum is. More details about DDS-based PLL will be discussed in section 3.3.



(a) PLL power spectrum when $f_{DDS}=10$ MHz



(b) PLL power spectrum when $f_{DDS}=12.5$ MHz

Figure 3.5 PLL power spectrum with different DDS signal

3.2 Phase-locked Loop Frequency Synthesizer

A Phase Locked Loop (PLL) is a fundamental part of radio, wireless and telecommunication technology. It is a simple negative feedback architecture that allows economic multiplication of crystal frequencies by large variable numbers. By studying the loop components and their reaction to various noise sources, we will show that PLL is uniquely suited for generation of stable, low noise tunable RF signals for radio, timing and wireless applications.

3.2.1 Working Principle of PLL Synthesizer

The phase locked loop is a closed-loop control system which is used for synchronization of the frequency and phase of a locally generated signal with that of an incoming signal. It is basically a nonlinear feedback loop. The PLL consists of a voltage controlled oscillator (VCO), a phase detector, serial dividers, and a loop filter. The PLL output frequency can synchronize with reference frequency by phase tracking of PLL. The diagram of PLL is shown in figure 3.6:

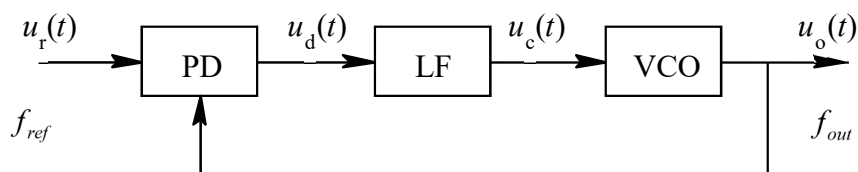
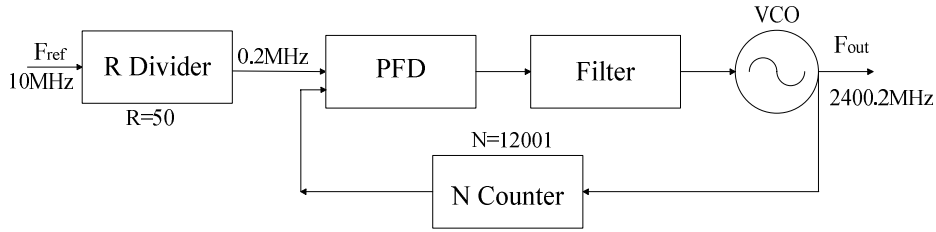
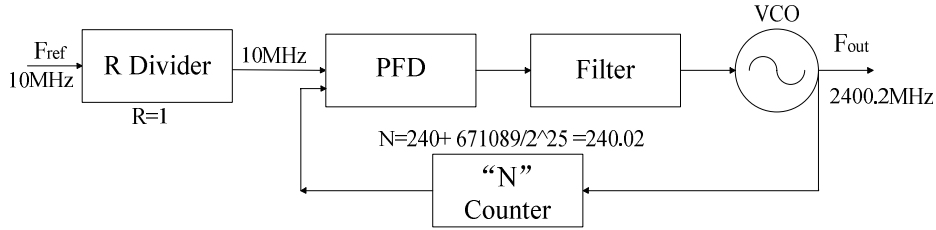


Figure 3.6 Diagram of a phase locked loop

The basic method of an integer-N phase-locked frequency synthesis is: the phase locked loop locks a high stable reference oscillator, and a programmable divider is in the loop. We change the divider ratio by programming to get stable output frequency which is N times the reference frequency. Figure 3.7(a) shows the diagram of an integer-N PLL when reference frequency is 10 MHz and output frequency is 2400.2 MHz.



(a) Diagram of an integer-N PLL



(b) Diagram of a Fractional-N PLL

Figure 3.7 Comparison between integer-N PLL and Fractional-N PLL

When the loop is locked, the output frequency is:

$$F_{out} = \frac{N}{R} F_{ref} \quad (3.8)$$

An unavoidable occurrence in digital PLL synthesis is that frequency multiplication (by N), raises the signal's phase noise by $20 \log_{10}(N)$ dB. The phase detectors are typically the dominant source of close-in phase noise, N becomes a limiting factor when determining the lowest possible phase noise performance of the output signal. We could reduce the close-in phase noise of our system by reducing the value of N but unfortunately the channel spacing of an integer- N synthesizer is dependent on the value of N .

A phase detector is a digital circuit that generates high levels of transient noise at its frequency of operation, F_p . This noise is superimposed on the control voltage to the VCO and modulates the VCO RF output accordingly. This interference can be viewed as spurious signals at offsets of $\pm F_p$ (and its harmonics) around F_{vco} . To prevent this unwanted spurious noise, a filter at the output of the charge pumps (called the loop filter) must be present and appropriately narrow in bandwidth. Unfortunately, as the loop filter bandwidth decreases, the time required for the synthesizer to switch between channels increases.

If N could be made much smaller, F_p would increase and the loop filter bandwidth

required to attenuate the reference spurs could be made large enough so that it does not impact the required switching speed of our system. Once again, however, the upper limit of F_r is bound by our channel spacing requirements. This illustrates how our desires to optimize both switching speed and spur suppression directly conflict with each other.

Fractional PLL technology has made it possible to alter the relationship between N , F_r , and the channel spacing of the synthesizer. [28] It is now possible to achieve frequency resolution that is a fractional portion of the phase detector frequency. This is accomplished by adding internal circuitry that enables the value of N to change dynamically during the locked state. If the value of the divider is “switched” between N and $N+1$ in the correct proportion, an average division ratio can be realized that is N plus some arbitrary fraction, K/F . This allows the phase detectors to run at a frequency that is higher than the synthesizer channel spacing.

$$f_{out} = (INT + \frac{K}{F}) \times f_{ref} \quad (3.10)$$

where, F = the fractional modulus of the circuit, K = the fractional channel of operation.

Figure 3.7 (b) shows the diagram of the fractional-N PLL frequency synthesizer. Comparison with 3.7 (a), it can be seen that fractional-N PLL allows larger reference frequency values, which results in a smaller multiplier term N . Since the PLL's phase noise is multiplied by the value of N chosen and frac-N PLLs require smaller values for N , the phase noise increase due to multiplying the reference frequency by N will decrease by $20 \log_{10}(N)$ dB. Another advantage is the smaller step-size or higher resolution. A frac-N allows step sizes on the order of tens of Hertz, while an integer-N may result in tens of kilohertz. The frac-N also will lock faster when compared to a similar integer-N solution. This is because the lower value of N allows a wider loop filter bandwidth, which in turn allows a faster lock time. And the biggest disadvantages of a frac-N PLL are the fractional and integer boundary spurs it generates, its increased complexity from a usage standpoint.

3.2.2 Phase Noise Analysis

Phase noise of PLL is a random process. Although we can use simulation software such as ADIsimPLL for analysis, we need to begin with the linearized PLL model, which is shown in figure 3.8 [29] :

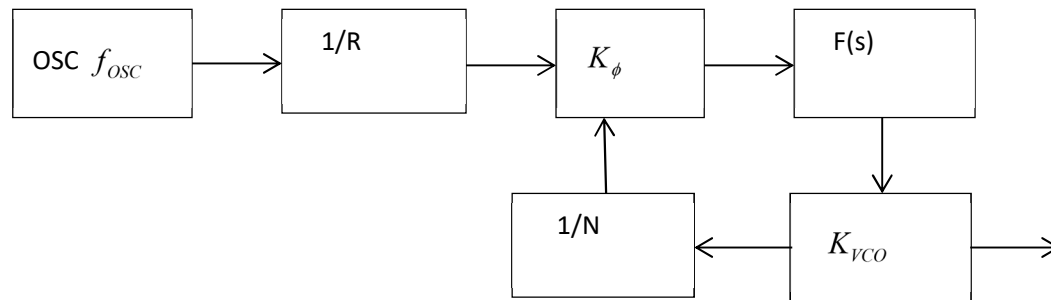


Figure 3.8 Linearized PLL model

Where $F(s)$ is transfer function of loop filter, K_ϕ is phase detector sensitivity, K_{VCO} is VCO sensitivity. From the PLL phase noise model, forward passage gain and reverse gain can be expressed as: $G(s) = \frac{K_\phi K_{VCO} F(s)}{s}$ and $H = \frac{1}{N}$.

We take the reference crystal oscillator as an example to derive the transfer function of each noise source: assume $\theta_{osc}(s)$ is phase noise generated by reference crystal oscillator and ignore the input of other noise sources:

$$\left(\frac{\theta_{osc}(s)}{R} - \frac{\theta_{out}(s)}{N}\right) K_\phi F(s) \frac{K_{VCO}}{s} = \theta_{out}(s) \quad (3.11)$$

According to the equations of forward gain and reverse gain, the transfer function of reference crystal oscillator can be written as:

$$T(s) = \frac{\theta_{out}(s)}{\theta_{osc}(s)} = \frac{1}{R} \frac{G(s)}{1 + G(s)H} \quad (3.12)$$

Table 3.1 Transfer function of noise components in PLL

Noise sources	Transfer function
Crystal Oscillator	$\frac{1}{R} \frac{G(s)}{1 + G(s)H}$
R Divider	$\frac{G(s)}{1 + G(s)H}$

N Divider	$\frac{G(s)}{1+G(s)H}$
Phase Detector	$\frac{1}{K_\phi} \frac{G(s)}{1+G(s)H}$
VCO	$\frac{G(s)}{1+G(s)H}$

From the table 3.1 shown above, we can notice that transfer functions of phase detector, R divider, N divider and crystal oscillator contain a same factor: $\frac{G(s)}{1+G(s)H}$. So these noise sources are collectively called in-band phase noise. To analyze this problem, phase margin ϕ are defined in equation (3.11), it determines stability as in other feedback loops:

$$180^\circ - \angle G(j\omega_o)H = \phi \quad (3.11)$$

Using these definitions and equations about forward passage gain and reverse gain, we can get, ω_o is the loop bandwidth:

$$\frac{G(s)}{1+G(s)} \approx \begin{cases} N & \text{when } \omega \ll \omega_o \\ G(s) & \text{when } \omega \gg \omega_o \end{cases} \quad (3.12)$$

Otherwise, the transfer function of VCO is $\frac{G(s)}{1+G(s)H(s)}$, and it can be expressed approximately as:

$$\frac{G(s)}{1+G(s)} \approx \begin{cases} \frac{N}{G(s)} & \text{when } \omega \ll \omega_o \\ 1 & \text{when } \omega \gg \omega_o \end{cases} \quad (3.13)$$

Thus, as it shown in Figure 3.9, the in-band noise of PLL ($\omega \ll \omega_o$) mainly depends on crystal oscillator, phase detector and divider, and the out-band noise ($\omega \gg \omega_o$) depends on VCO. [30]

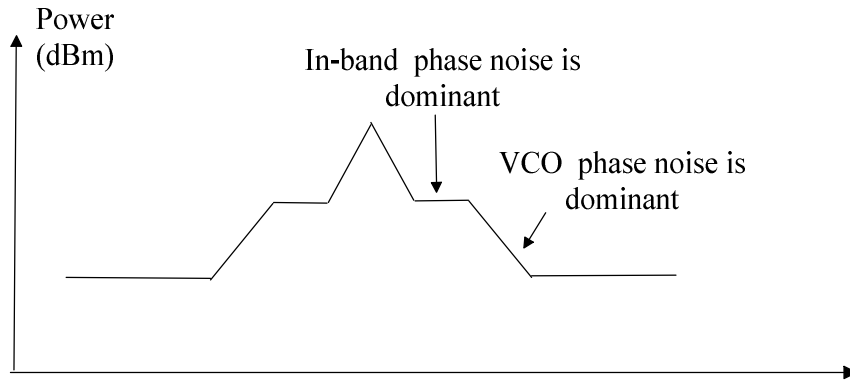


Figure 3.9 Phase noise spectrum of PLL

Besides, the frequency divider in the feedback path may have a significant contribution to the total phase noise of the PLL depending on its implementation and other properties of the loop. One of the cardinal principles is that multiplication by N causes loss of $20\log_{10}(N)$ in phase noise performance; division improves by the same number. If a 100 kHz crystal signal is multiplied by PLL (or any other way) to 1000 MHz, the multiplication ratio is 10,000 and the corruption in phase noise will be 80 dB. When divided down by a digital divider, the divider improves jitter by N times or $20\log_{10}(N)$ in noise power.

In this thesis, we choose ADF4158 PLL chip, it is fractional-N PLL frequency synthesizer, of which RF bandwidth is up to 6.1 GHz, and it contains a 25-bit fixed modulus allowing subhertz resolution at 2.4 GHz. Figure 3.10 shows the triangle frequency modulation measured by real time analyzer DSO804A. From figure 3.10, we can find that ADF4158 PLL generates a continuous wave from 2.4 to 2.5 GHz with a period of 1.06 ms.

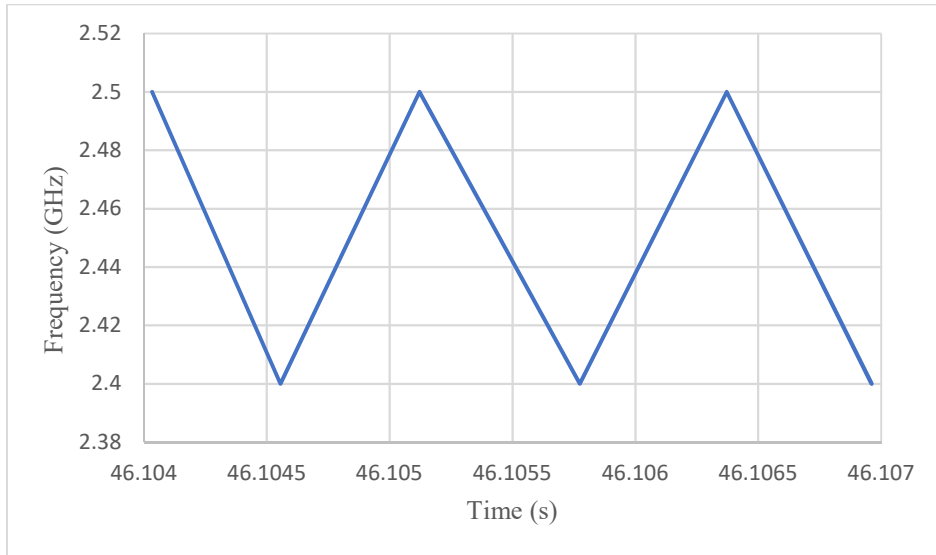


Figure 3.10 ADF4158 time domain measurement

Figure 3.11 show the output signal power spectra when $N=192$ and $N=1920$: the loop bandwidth is 100 kHz when $N=192$ and loop bandwidth decreases to 20 kHz when N increases to 1920. We can find that the signal power spectrum with smaller N has wider loop bandwidth and better in band phase noise:

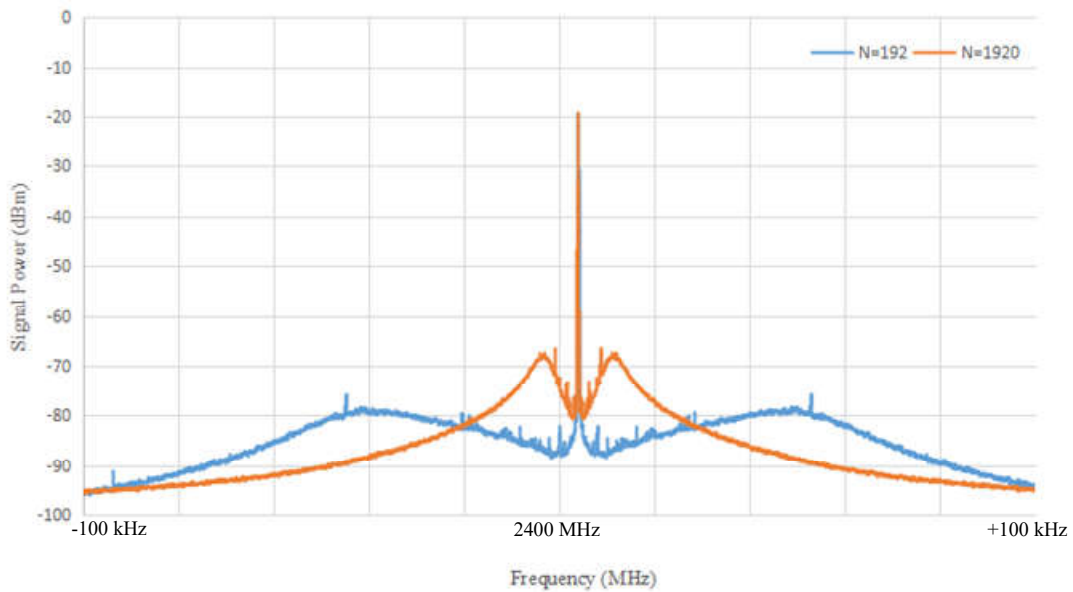


Figure 3.11 PLL power spectrum with different N

3.3 DDS-based PLL Synthesizer

Direct digital frequency synthesizer technology and phase-locked loop frequency

synthesis technology have their own advantages and disadvantages. DDS has the advantage of quick switching time and low phase noise; the disadvantage is the low frequency, and the spectrum quality is poor. PLL is characterized by high output frequency, good quality spectrum; the drawback is the low frequency switching speed. The design requirements can be achieved by combining these two techniques considering bandwidth, frequency accuracy, switching time, phase noise, and spurs.

In this thesis, we use ADF 4158 evaluation board as the PLL frequency synthesizer and use AD9833 DDS board as reference frequency to replace the TCXO chip on PLL board. TCXO is a temperature compensated crystal oscillator. Compensation components have been added to enhance the temperature stability of the basic oscillator. Compared to TCXO, a major advantage of a DDS system is that its output frequency and phase can be precisely and rapidly manipulated under digital processor control. so that we can choose a high PFD frequency with good power spectrum for PLL.

Figure 3.15 shows the phase noise and different loop bandwidth with different N of ADF4158 PLL chip, the formula for the single sideband (SSB) phase noise in dBc/Hz can be written as: $L(fm) = P_{SSB}(dBm) - 10 \log(RBW) - P(Carrier)(dBm)$.

We can find that with the increase of N, loop bandwidth decreases. As discussed in section 3.2.2 and 3.2.3, wider loop bandwidth means smaller in-band phase noise. Thus, for better phase noise, we set $f_{DDS} = f_{ref} = 12.5\text{MHz}$ and $R=1$ in R counter and enable the reference doubler, thus the PFD frequency is 25 MHz. To generate frequency range from 2400 MHz to 2500 MHz, the frequency synthesizer begins with:

$$\left(96 + \frac{0}{2^{25}}\right) \times 25\text{MHz} = 2400\text{MHz} \quad (3.15)$$

and ends with:

$$\left(100 + \frac{0}{2^{25}}\right) \times 25\text{MHz} = 2500\text{MHz} \quad (3.15)$$

As discussed in section 3.2, N causes increase of $20 \log_{10}(N)$ in phase noise performance. When $N=96$, phase noise will increase about 40 dB. Figure 3.14 shows in-band phase noise comparison between DDS and DDS-based PLL, we can find that the in-band phase noise of PLL is about 40 dB larger than phase noise of DDS.

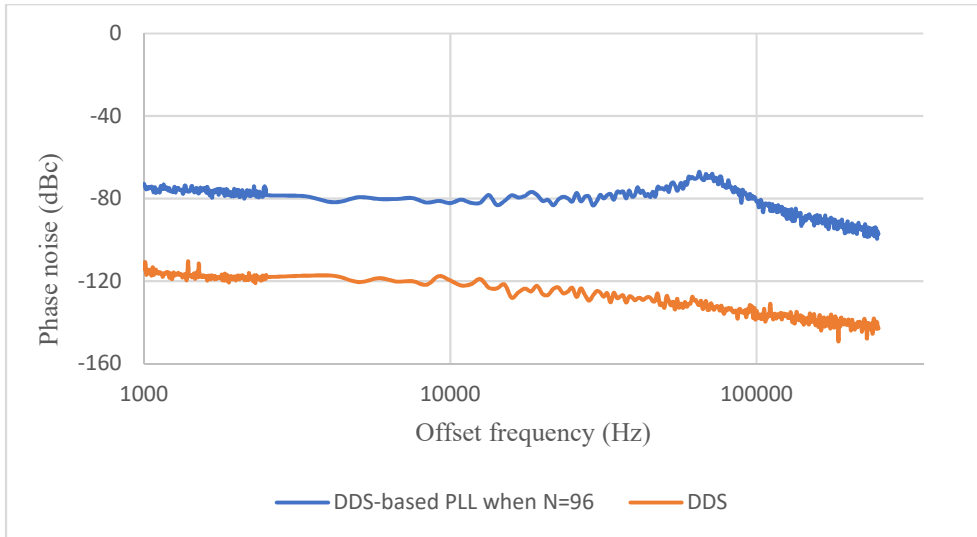


Figure 3.14 Phase noise comparison between DDS and DDS-based PLL when N=96

N changes from 96 to 100, and the minimum resolution is $f_{\text{PFD}} / 2^{25} = 0.3725$ Hz. At this time, loop bandwidth is about 136 kHz and phase noise is -85 dBc/Hz@1 kHz.

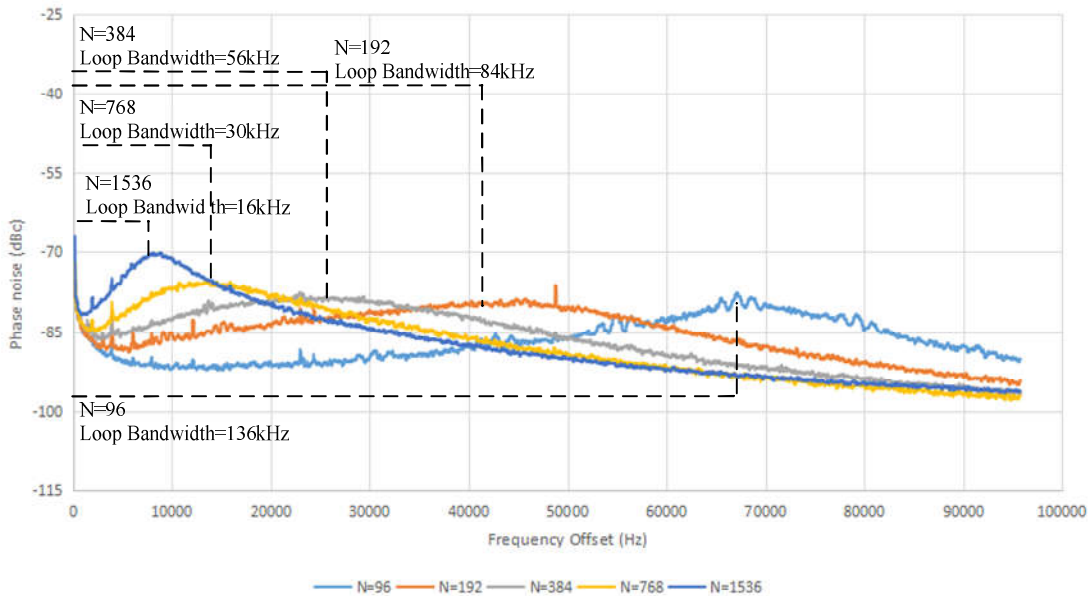


Figure 3.15 Phase noise measurement (measured by power spectrum analyzer Agilent E4440A, RBW=100 Hz, VBW=10 Hz)

As discussed in chapter 2, the IF bandwidth is 40 kHz, and PLL phase noise is about -95 ~ -85 dBc/Hz. And according to measurement in chapter 4, IF signal power is -40 dBm when object is 0.45 m far from the radar and IF power is about -95 dBm when R= 10 m. Thus, such phase noise is much smaller than IF power when object is

close. And phase noise sources in a primary radar (phase noise from RF and LO signals) are correlated and as a result, the phase noise will partially cancel out due to range correlation effects as shown in [24]. So in chapter 4, the thesis will focus on how receiver system noise and gain influence the performance of the radar transceiver.

3.4 Summary

The comparative discussion consists of PLL, DDS and DDS-based PLL. We discuss the working principle of DDS and PLL, and a DDS-driven PLL frequency synthesizer architecture is given in this chapter. We also talk about some main parameters for frequency synthesizer, particularly phase noise and spurs. And do the measurement about phase noise of PLL board and DDS-based PLL board. The measurement proves that the design of DDS + PLL frequency synthesizer adopts DDS driving PLL generate RF signals and the generated frequency is stable, reliable. The signal amplitude and phase noise can be up to the requirements of FMCW radar transceiver. Next the DDS+PLL frequency synthesizer is put into use.

Chapter 4

FMCW Radar System Design and Test

In this thesis, we use a homodyne receiver with one output signal. After being amplified by a power amplifier, the transmitting signal is received by the homodyne receiver: incoming RF signal is down-converted to baseband (zero frequency) in one step by mixing with an oscillator output of the same frequency. The resulting baseband signal is then filtered with a low-pass filter to select the desired channel. To improve the input and output matching of LNA, we add two isolators in the receiver. This is illustrated in the block diagram in figure 4.1.

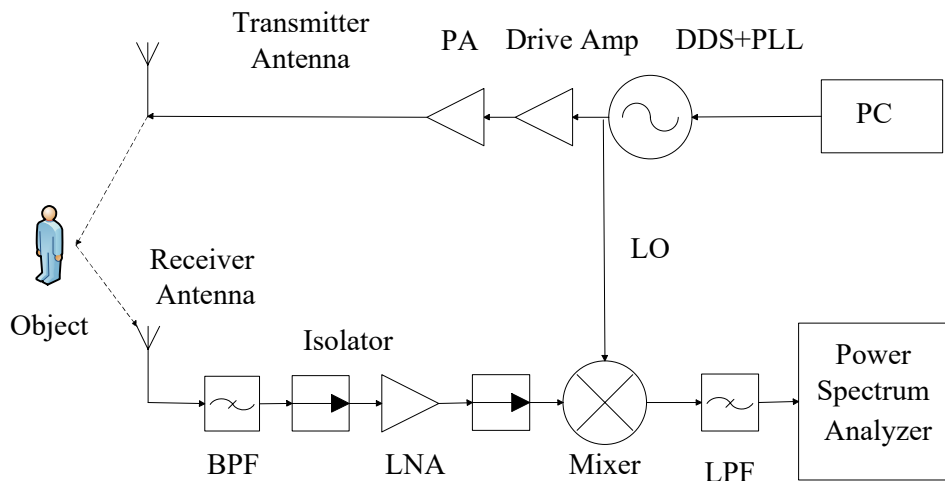


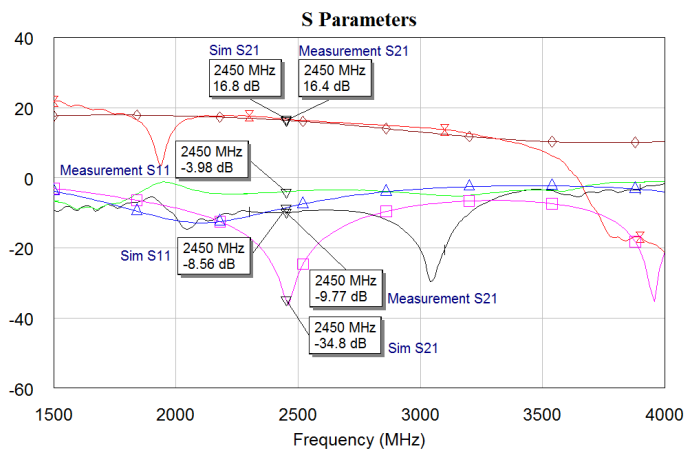
Figure 4.1 Simplified block diagram of radar transceiver

This thesis calculates distance information by IF signals from power spectrum analyzer instead of FFT. And this radar still shows the good performance to position and track objects in short range.

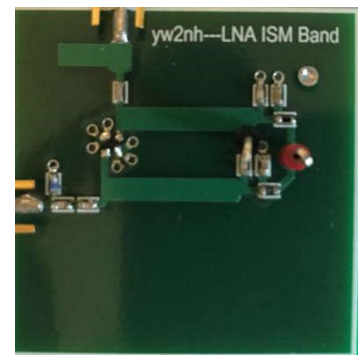
4.1 Radar System Design

4.1.1 LNA design and test

In this thesis, we describe how to design a microwave LNA at 2.4 GHz starting from a BJT transistor chip to the actual board layout. The transistor used is the Freescale Semiconductor Transistor, part BFU760F, which is a NPN wideband silicon germanium RF transistor. This transistor is characterized as follows at the quiescent operating point with targeted frequency of 2.4 GHz. The load line and S matrix are determined through simulations. This resulted in unilateral operation of the transistor which implies a simpler matching network because there is limited internal transistor feedback. Source and load matching networks are designed at 50 Ohms with the corresponding S matrix. Stability was simulated and proven to be stable for the specified biasing range of the part. In the measurement shown in figure 4.2, the gain of our amplifier circuit is 16.4dB at 2.45 GHz, which is close to the simulation. Noise figure is measured by spectrum analyzer and a noise source NC3101. At 2.5 GHz, NF is 2.3 dB.



(a) S parameters of LNA



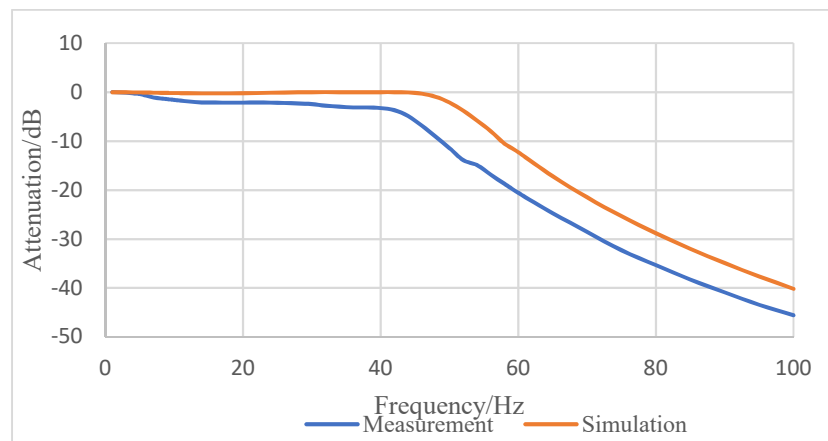
(b) Picture of LNA

Figure 4.2 Measurement of LNA

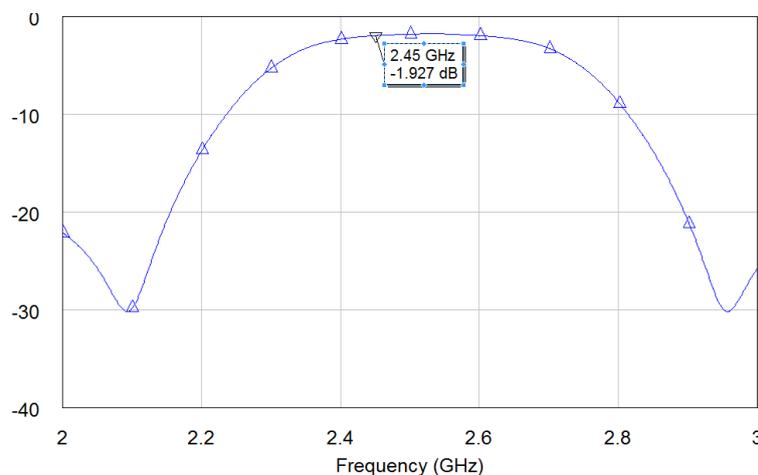
4.1.2 Filter design and test

The low pass filter only allows low frequency signals from 0 Hz to its cut-off frequency to pass while blocking those any higher. In this thesis, we design a maximally flat low-pass filter with a cutoff frequency of 40 kHz, impedance of 50 Ohm, and at least 10 dB insertion loss at 50 kHz and 40 dB insertion loss at 100 kHz.

The high pass filter only allows high frequency signals from its cut-off frequency, while blocking those any lower. And the band pass filter allows signals falling within a certain frequency band setup between two points to pass through while blocking both the lower and higher frequencies either side of this frequency band, [25]. The parallel coupled transmission lines are used to construct band-pass filter, whose the passband is 2.4 GHz to 2.5 GHz. The results of two filters are shown in figure 4.3.



(a) Attenuation of LPF



(b) Attenuation of BPF



(c) Picture of LPF and BPF

Figure 4.3 Filter attenuation

4.1.3 Mixer Test

A mixer is a three-port device that uses a nonlinear or time-varying element to achieve frequency conversion. An ideal mixer produces an output consisting of the sum and difference frequencies of its two input signals. Operation of practical RF and microwave mixers is usually based on the nonlinearity provided by either a diode or a transistor. In this thesis, we need a frequency down-conversion mixer in the radar receiver, the desired IF output in a receiver is the difference frequency, which can be easily selected by low-pass filtering: $f_{IF} = f_{RF} - f_{LO}$.

This work adopts a double-balanced mixer, which uses two hybrid junctions or transformers, and provides good isolation between all three ports, as well as rejection of all even harmonics of the RF and LO signals. [30] This leads to very good conversion loss, but less than ideal input matching at the RF port. The double-balanced mixer also provides a higher third-order intercept point than either a single-ended mixer or a balanced mixer.

An important figure of merit for a mixer is therefore the conversion loss, which is defined as the ratio of available RF input power to the available IF output power, expressed in dB:

$$L_c(dB) = P_{RF} - P_{IF} \quad (4.1)$$

In this thesis, we use LTC5548 microwave double balanced passive mixer, its main parameters are shown in table 4.1:

Table 4.1 Main Parameters of LTC5548 Mixer

Parameters	Values
Conversion Loss	6.2 dB @ RF input =2.4 GHz
Noise Figure	7 dB @ RF input =2.4 GHz
Input P1dB Compression	16 dBm
LO to RF Leakage	< -25 dBm
LO to IF Leakage	< -25 dBm

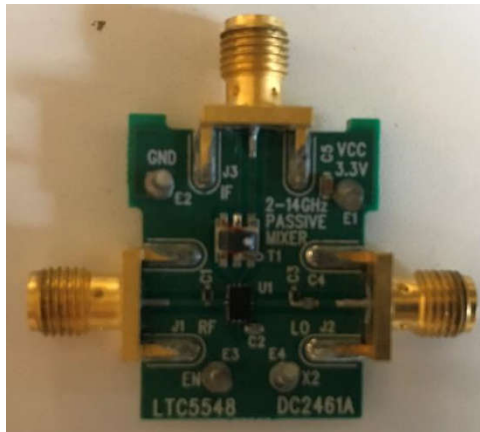
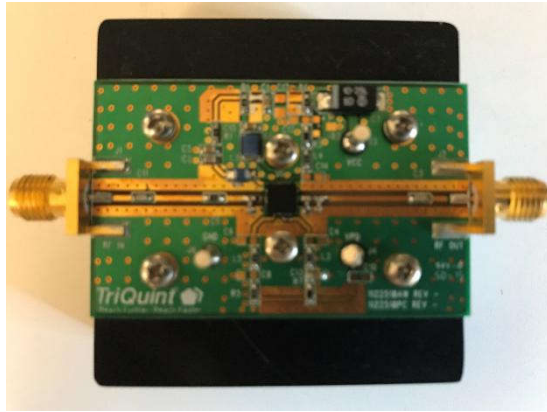


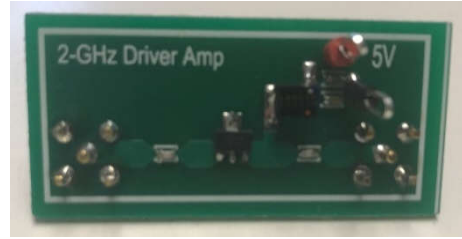
Figure 4.4 Picture of mixer

4.1.4 Power Amplifier Test

RF power amplifiers are used to increase the output power in a wide variety of applications including wireless communication, TV transmissions, radar, and RF heating. The thesis adopts the MMG3H21NT1 broadband high linearity amplifier chip and TQP9111 power amplifier chip. MMG3H21NT1 is a general purpose amplifier, which has 12.6 dB small-signal gain, 5.4 dB input return loss and 10.4 dB output return loss. TQP9111 is a high efficiency two-stage driver amplifier in a low-cost surface-mount package. This linear amplifier integrates two high performance amplifier stages onto a module to allow for a compact system design. The integrated inter-stage match minimizes performance variation that would otherwise be attributed to external matching component value and placement tolerances. At 2.4 GHz, this PA has 13 dB input return loss, 20 dB output return loss, 29.8 dB gain and 32.5 dBm 1dB compression point.



(a) Power amplifier



(b) Drive amplifier

Figure 4.5 Picture of amplifiers

4.1.5 Antenna Test

In this radar system, we adopt two monopole antennas as transmitting and receiving antennas. Main parameters of the antennas are shown in table 4.2. Return loss is measured by VNA. Antenna gain is cited in the datasheet of monopole antenna GW.05.0153.66666

Table 4.2 Main Parameters of antenna

	2400 MHz	2450 MHz	2500 MHz
Average gain (dBi)	-2.62	-2.61	-1.74
Efficiency (%)	54.71	54.78	67.05
Peak gain (dBi)	1.04	1.25	0.82
Return loss (dB)	<-6	<-6	<-6



Figure 4.6 Picture of antenna

4.1.6 Radar Components Summary

In this chapter, we designed each component of the homodyne radar receiver, including low-noise amplifier, band-pass filter, low-pass filter, mixer and power amplifier, the summary is shown in table 4.3. In this system, total noise and gain is shown below:

$$NF_{total} = 10 \log_{10} \left(n_1 + \sum_{i=2}^3 \frac{n_i - 1}{\prod_{j=1}^{i-1} g_j} \right) = 3.529 \text{ dB} \quad G_{total} = \sum G_i = 9.2 \text{ dB}$$

Table 4.3 Summary of Radar Components

Component Name	Main Parameters
Low-noise amplifier	S11= -3.98 dB S22= -9.77 dB S21= 16.4 dB NF=2.3 dB @2.45 GHz
Band-pass filter	Passband= 2.4-2.5 GHz Loss= 1.93 dB
Low-pass filter	Passband= 0-40 kHz
Mixer	Down Converter NF=7 dB Conversion Loss =6.2 dB @2.45 GHz
Drive Amplifier	S11= -5.4 dB S22= -10.4 dB S21= 12.6 dB @2.45 GHz
Power Amplifier	Power gain=29.8 dB S11= -13 dB, S22= -20 dB @2.45 GHz
Isolator	Loss=0.18 dB
Antenna	Average gain=-2.62 dBi @2.4 GHz Return loss<-6 dB

4.2 Human indoor positioning and tracking



Figure 4.7 Radar test in the aisle in Thornton Hall

The radar receiver is tested in the aisle in Thornton Hall, and the attenuation and reflection of wall and electrical devices will affect the results, particularly when the transmitting signal is weak.

In this test, we use a power spectrum analyzer Agilent E4440A to measurement. The measurement range is from -5-40 kHz and there are 600 samples in this range. Figure 4.8 with blue line shows the IF power spectrum when there is no objective in the front of radar system. It can be seen that there are spurs in the spectrum resulting from reasons shown below:

(1) Receiver mismatch: The input and output return loss of LNA is not very good, which means that signal may bounce between LNA and BPF. Such oscillation means there will be more than one RF frequency for the mixer RF input, and finally results in inter-modulation of the mixer. Besides, the receiver may suffer even-order distortion. When there are two strong frequencies ω_1 and ω_2 at the input of LNA, it will generate a low-frequency beat $\omega_1 - \omega_2$. Since the isolation is finite from the RF input to the IF output, such low-frequency beat will appear in the IF port.

When the LNA is removed, we can find that spurs still exist but are decreased significantly. Besides, when we use lossless cables to replace antennas and objects, the power of spurs increases. If we add an attenuator at the input of BPF, the spurs power decreases. Thus, it can be proved that the radar receiver generates spurs. To solve this problem, we add two isolators at the input and output of LNA. The comparison between IF frequency without isolators and IF frequency with isolators is shown in figure 4.8.

The red curve is power spectrum after adding isolators, we can find that the quality of spectrum improves because of isolators.

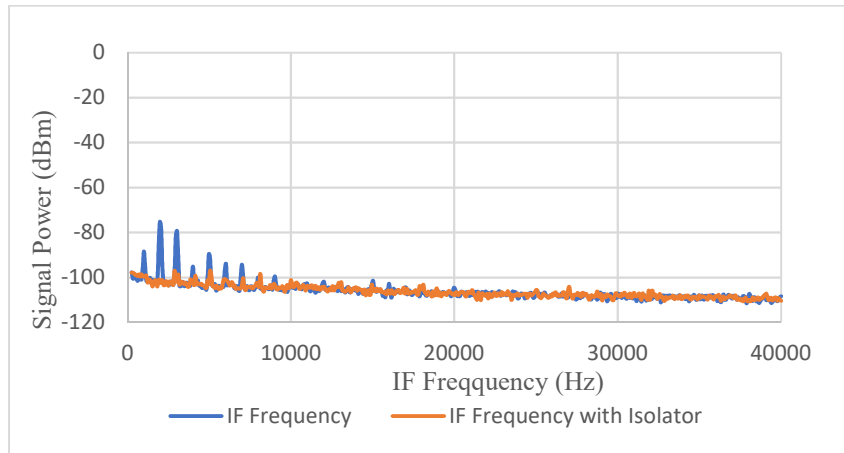


Figure 4.8 Spectrum comparison between IF with isolators and IF without isolators

(2) LO leakage and DC offset: When the isolation between the LO port and the inputs of the mixer is not infinite, LO signals can leak to mixer RF port and LNA input, finally leak to the receiving antenna. Such LO leakage is received by mixer RF port and mixed with LO. It is called DC offset because such frequency beat is zero. When the transmitting antenna is removed and the radar receiver works (no RF signal), spurs decreases but still exist, which is shown in figure 4.9. Thus, LO leakage can generate spurs, but it is not the main reason in this system.

Besides, we also need to consider LO phase noise, [37]. The noise source of LO and RF signals are correlated and as a result, the phase noise partially cancels out due to range correlation effects.

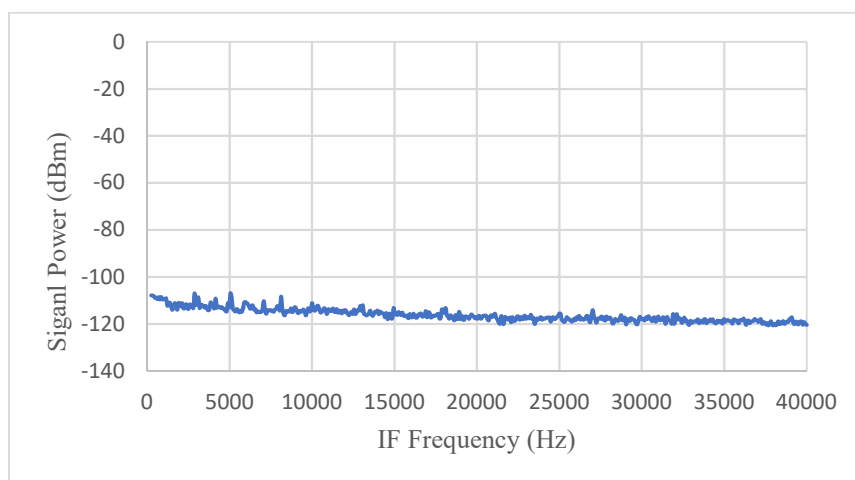
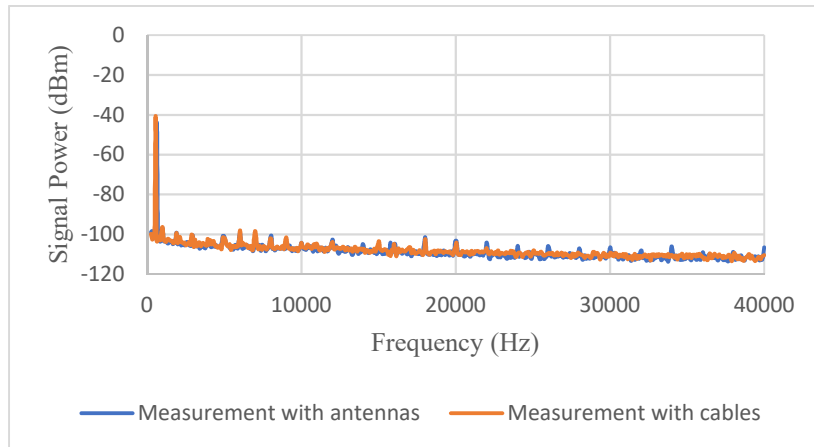
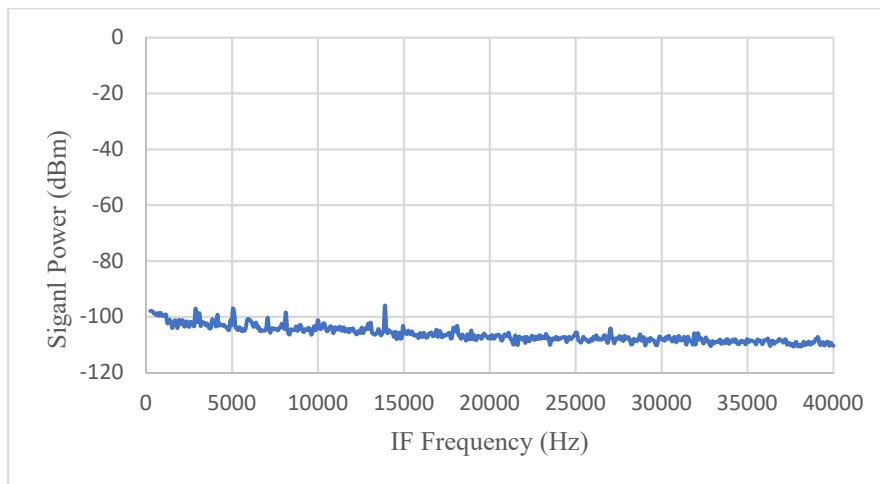


Figure 4.9 IF spectrum with LO leakage (antennas are replaced by 50 Ω termination)

(3) Reflection: the reflection from the environment can also generate spurs. The radar system is tested in an empty aisle for weak reflection. But multireflection still generates spurs, particularly when the object is close to radar system. Multireflection can generate more than one RF signal and result in mixer inter modulation: when more than one RF signals, f_1 and f_2 , go into mixer RF port, spurs $\pm[(rf_1 - sf_2) - f_{LO}]$ will be generated periodically.



(a) IF signal when $R= 0.45$ m measured in the aisle ($IF=600$ Hz, $IF_{Measurement}=625$ Hz)



(b) IF signal when $R= 10$ m in the aisle

($IF=13333$ Hz, $IF_{Measurement}=13600$ Hz)

Figure 4.10 IF signal spectrum

Figure 4.10 (a) and (b) shows this IF power difference when $R= 0.45$ m and $R= 10$ m. The thesis makes a control experiment: a person stands in the front of radar transceiver and holds a copper plate to enhance reflection, the IF power spectrum is

recorded after the result is stable. After that, we use cables with the same distance to measure it again, the IF spectrum in the “pure environment” is recorded again. The two data can be compared to check the accuracy of the radar. All data can be checked in appendix. After range is larger than 10 m, the effective IF signal is inundated in spurs and noise. After calculation, we can find that there is difference between calculation and real range information. With the increase of range, such error increases and positioning accuracy decreases. Figure 4.11 plots the error distribution with 10 times measurement, as shown in the figure, the maximum error for all the tests is about 30 cm, and maximum standard deviation is 7cm (The y axis for distance is on the left and the y axis for standard deviation is on the left). This distance detection accuracy is sufficient for indoor localization purposes.

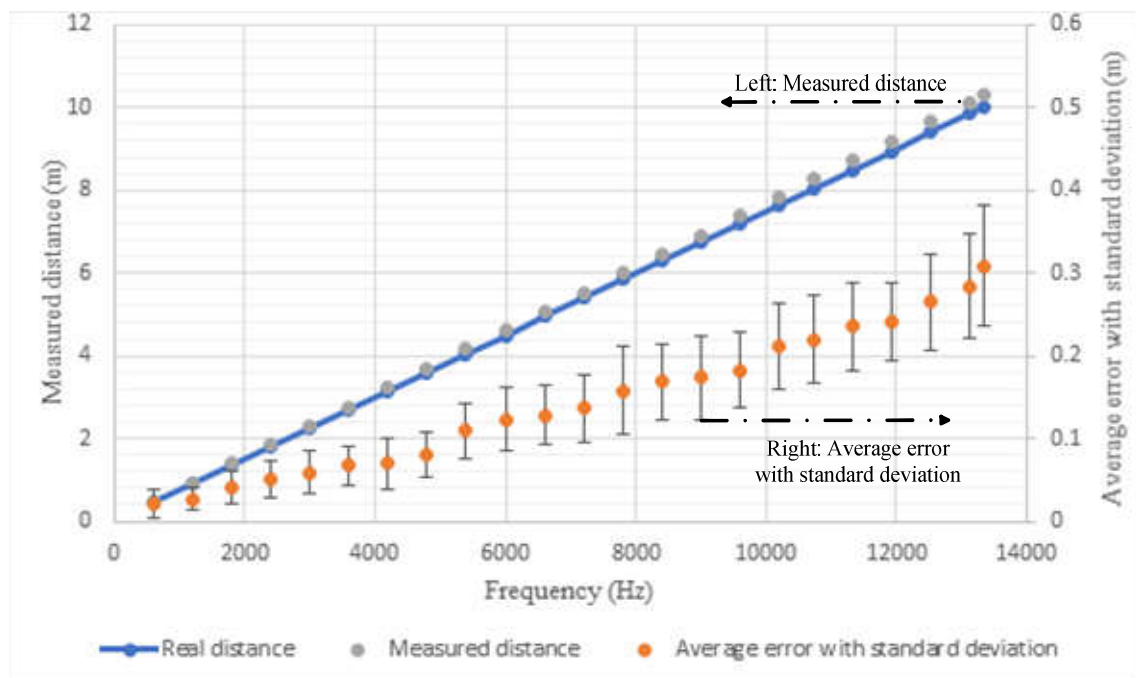


Figure 4.11 Range measurement

4.3 Analysis and Future Work

It’s necessary for us to discuss about ideal maximum detection range: the radar range equation represents the physical dependences of the transmit power, that is the wave propagation up to the receiving of the echo-signals.

$$R_{\max} = \sqrt[4]{\frac{P_t G_t G_r \lambda^2 \sigma}{(4\pi)^3 P_{\min}}} \quad (4.2)$$

where P_t is transmit power, G_t and G_r are transmitting and receiving antenna gain, λ is transmit wavelength, σ is target radar cross section, P_{\min} is the minimum detectable signal.

The antenna gain is -2 dBi, wavelength is 0.12 m and radar cross section is a 0.3×0.3 m copper plate. $P_{\min} = k(T_a + T_{\text{receiver}} + T_{\text{analyzer}})B \cdot (SNR)_{\min}$, where T_a is antenna noise temperature, T_{receiver} is receiver noise temperature and T_{analyzer} is spectrum analyzer noise temperature.

Since it's hard to calculate antenna noise temperature, we design an experiment to measure it, which is shown in figure 4.10. First, we connect the noise source NC3011 to spectrum analyzer to get noise power P_o , and then turn on the noise source to get noise power P_H . We can get ENR of the noise source from data sheet and calculate noise temperature of noise source T_{noise} :

$$ENR = \frac{T_{\text{noise}}}{T_o} - 1 = 15.29 \text{ dB} = 33.8 \rightarrow T_{\text{noise}} = 34.8 T_o \quad (4.3)$$

where T_o is room temperature.

And we can get Y factor:

$$Y = \frac{P_H}{P_o} = 3.64 \quad (4.4)$$

Thus, noise temperature of spectrum analyzer is:

$$F_{\text{analyzer}} = \frac{ENR}{Y - 1} = 12.8 = 11.1 \text{ dB} \quad (4.5)$$

$$T_{\text{analyzer}} = (F_{\text{analyzer}} - 1)T_o = 11.8 T_o \quad (4.6)$$

Note that the analyzer shown in (4.6) is measured at 2.4 GHz and cannot be used in radar equation (4.2) because the IF frequency is 0-40 kHz.

Then we use antenna to replace noise source and get noise power P_H' . Since we use the same resolution bandwidth and reference level, we can get:

$$\frac{P_H'}{P_H} = \frac{k(T_{antenna} + T_{analyzer})B}{k(T_{noise} + T_{analyzer})B} = \frac{T_{antenna} + T_{analyzer}}{T_{noise} + T_{analyzer}} \quad (4.7)$$

$$\Rightarrow T_{antenna} = \frac{P_H'}{P_H}(T_{noise} + T_{analyzer}) - T_{analyzer} = 9.17T_o$$

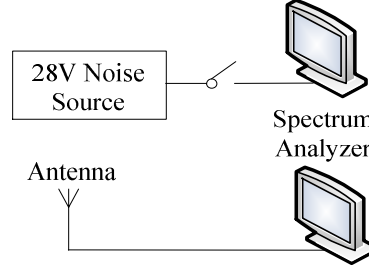


Figure 4.10 Antenna temperature measurement

Next, we need to discuss about parameters of spectrum analyzer since we use the spectrum analyzer instead of FFT algorithm: Resolution bandwidth also affects sensitivity. The ideal RBW has a flat passband and infinite attenuation outside that passband. But it must also have good time domain performance so that it behaves well when signals sweep through the passband. The spectrum analyzer in this thesis uses four-pole synchronously tuned filters for their RBW filters. The response of the filter to noise of flat power spectral density will be the same as the response of a rectangular filter with the same maximum gain and the same area under their curves. The width of such a rectangular filter is called the equivalent noise bandwidth of the RBW filter. The ratio of the equivalent noise bandwidth to the resolution bandwidth is 1.128.

The input attenuator also affects the location of a true input signal on the display. Signals present at the analyzer input remain stationary on the display as we change the input attenuator, while the displayed noise moves up and down. Thus, we get the best sensitivity by selecting minimum input attenuation.

The video filter can be used to reduce the amplitude fluctuations of noisy signals while at the same time having no effect on constant signals. It should be noted that the video filter does not affect the average noise level and so does not, by this definition, affect the sensitivity of an analyzer.

Then we assume SNR_{min} is 5 dB, and $T_{antenna} = 9.17T_o$, $T_{receiver} = 1.25T_o$ calculated by noise figure of receiver. Since we don't have noise source at 40 kHz and cannot know the noise temperature of spectrum analyzer at IF frequency, we use noise temperature at 2.4 GHz to replace it. In this assumption, we can calculate the minimum

power that the antenna can receive:

$$(P_{in})_{min} = k(T_a + T_{receiver} + T_{analyzer}) \cdot B \cdot (SNR)_{min} \quad (4.8)$$

Thus, the minimum power that the spectrum analyzer can receive is:

$$(P_{out})_{min} = (P_{in})_{min} (dBm) + G(dB) = -140dBm \quad (4.9)$$

Thus, according to radar equation (4.2), we can calculate the maximum detectable range. R_{max} is 20 m when $(P_{out})_{min} = -140dBm$.

In the measurement, the maximum range is 10 m. The difference between calculation and measurement is resulted by assumed noise temperature and spectrum analyzer. Large RBW will increase the noise floor of the spectrum analyzer. Table 4.4 makes a summary of some problems and components which affect maximum detection range. Since we cannot get the precise value of ideal maximum detectable range, it is still necessary to analyze these parameters.

Table 4.4 Parameters which affects performance of FMCW radar

	Components	Description	Solution
Spectrum Analyzer	Attenuator	Input signals remain stationary and displayed noise moves up with the increase of attenuation.	Set minimum attenuation 0 dB
	Resolution Bandwidth (RBW)	The bandwidth of a flat band-pass filter. Smaller RBW is, higher frequency resolution is.	RBW=75 Hz
	Video Bandwidth	The video filter reduces the amplitude fluctuations of noisy signals but doesn't affect noise level.	VBW=10 Hz
	DC Offset	DC Offset is an offsetting of a signal from zero.	Blocking Capacitor
Receiver	Mismatch	When input and output return loss is not good, signal oscillates between components.	Use isolators
	Even-order Distortion	When there are two strong frequencies ω_1 and ω_2 at the input of LNA, a low-frequency beat $\omega_1 - \omega_2$ can be generated and leak to the IF port.	Use isolators
	Reciprocal Mixing	Reciprocal mixing results from the phase noise performance of the local oscillators.	Phase noise of LO is small enough to affect RF signals.

Receiver	Noise	It includes noise from antenna, devices in receiver and spectrum analyzer.	Decrease noise in receiver in future work, including loss of filters and noise of LNA.
	Gain	In this radar system, receiver gain is 9.2 dB	Increase receiver gain in future work, including gain of LNA and antenna efficiency.
Transmitter	LO Leakage	It results from finite isolation between RF and LO ports of the mixer.	In this radar receiver, isolation of the mixer is good.
	LO Phase Noise	Phase noise from LO may affect weak RF signals.	The phase noise of LO and RF signals are correlated and the phase noise partially cancels out.

This paper proposes a FMCW radar system at 2.4 GHz for intelligent housing system. In the part of frequency source, the thesis uses ADF4158 PLL chip to generate the 2.4 GHz continuous wave signal. It is the only PLL chip which can implement triangle frequency modulation at 2.4 GHz band from ADI. And in the thesis, a DDS chip is used as the reference frequency of PLL. Such DDS-based PLL frequency synthesizer provides an economic and efficient method to generate frequency modulated continuous wave at ISM band in small period with high linearity. Although the thesis has some discussion about phase noise and spurs, we still need do more research on decreasing phase noise and spurs. Table 4.5 shows some problems and components which affect maximum detection range.

Table 4.5 Performances summary and comparisons

Parameters	[31]	[32]	[33]	[34]	[35]	[36]	This work
Frequency source	N/A	DDS-based PLL	NI Signal Generator PXI3	DDS-based PLL	NA	PLL	DDS-based PLL
Center frequency	14.8 GHz	122 GHz	5.8 GHz	5.8 GHz	10.5 GHz	2.4 GHz	2.4 GHz
bandwidth	2 GHz	1 GHz	150 MHz	150 MHz	0.5 GHz	100 MHz	100 MHz
Modulation period	5 ms	2 ms	2 ms	1 ms	10 ms	NA	1 ms

Technology	65nm CMOS	PCB	PCB	PCB FR4	0.18 um CMOS	0.18 um CMOS	PCB FR4 ^[1]
TX output power	9 dBm	N/A	13 dBm	10 dBm	NA	-7 dBm	23 dBm
RX gain	30 dB	N/A	47.5 dB	40 dB	NA	24 dB	9.2 dB
RX noise figure	4.6 dB	N/A	N/A	N/A	11.5 dB	3.5 dB	3.5 dB ^[2]
Distance	10 m	2m	3ft-14ft	5 m	1-7.5 m	14 m	0.45-10 m
Average error	N/A	2 mm	0-5 cm	3-4 cm	4.9 cm	2.14 m	0.2-25 cm
Power Consumption	210 mW	NA	NA	NA	NA	NA	1.7 W

[1] We don't know what technology is used inside the DDS, PLL and mixer chip. LDMOS technology is used in power amplifier and drive amplifier in radar transmitter, and most parts in receiver, including LNA and filters are PCB.

[2] This noise figure only includes NF of receiver, doesn't include NF of power spectrum analyzer.

The comparison between the FMCW radar in this thesis and radars in other papers is shown in table 4.4. From the comparison, it can be seen that our advantages are economic and portable frequency source, and detection range is far enough for indoor position. Although we choose 2.4 GHz ISM band for less loss in FR4 PCB, we need higher frequency has less interference, for example, bluetooth and WiFi. Paper [31] adopts 65 nm CMOS technology and the transmitter and receiver

To implement human tracking and positioning for intelligent housing system, the FMCW radar system needs to have three abilities:

- 1) the ability to determine whether people comes in or goes out;
- 2) the ability of positioning and tracking;
- 3) the ability of velocity detection.

When the object moves, the power spectrum analyzer shows a fluctuation, which proves that the radar system can detect the movement of objects. According to the test shown above, the system shows the ability to detect the distance between radar and the object. As discussed in chapter 2, the velocity resolution depends on resolution bandwidth of spectrum and FMCW radar is not the best choice for velocity detection.

In conclusion, we need to make some improvements in future:

- 1) Improvements in device performance: I need to increase performance of LNA and BPF, decrease the noise of LNA and use material with less loss to replace

FR-4. And we need to use antennas with high gain. We also need a new design of LNA for better input and output return loss.

- 2) Improvements in receiver architecture: I need to build a homodyne receiver with two orthogonal I/Q signals in order to make the results more precise.
- 3) Research on indoor position algorithms: Since FMCW radar can only get the distance information between radar and object, we need range-based indoor position algorithms for human positioning, for example, triangulation method.

Besides, the IF signal is small because the distance between radar and object is small. Thus, the power at 0 Hz caused by DC will influence our observation and calculation. As it has been discussed in section 2.1, FMCW radar can detect velocity information. But the Doppler frequency shift for human walking is too small, which means that it's hard to distinguish f_b^+ and f_b^- from power spectrum. In order to get better range and velocity information, we can use two radars with different frequency range, which is shown in figure 4.11:

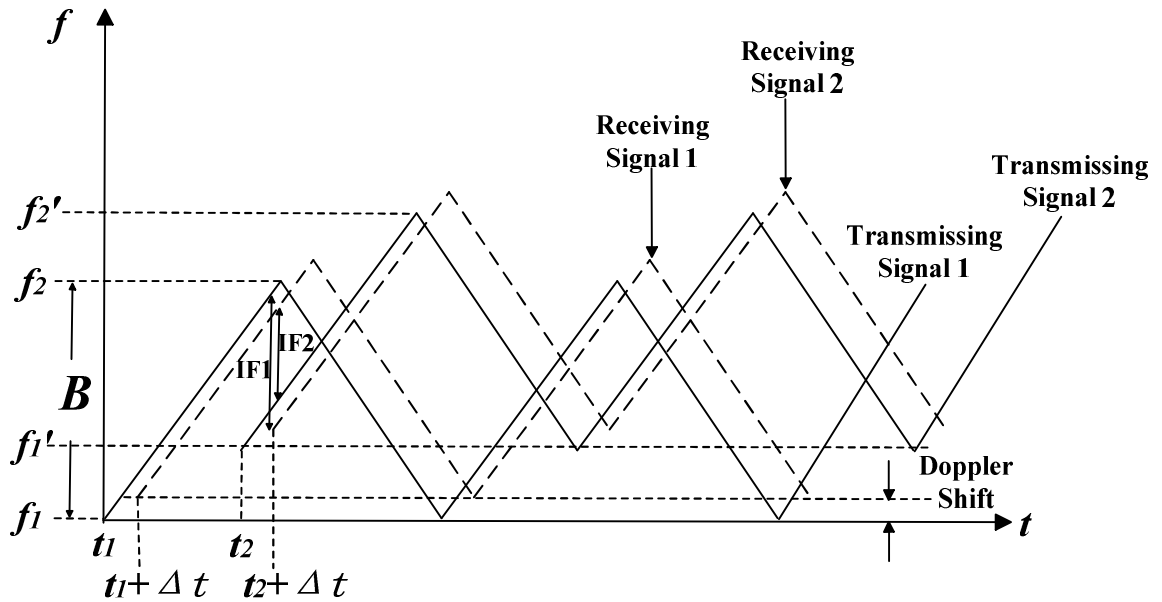


Figure 4.11 Range and velocity detection with two FMCW radars

In this radar system, $f_1 - f_2 = f'_1 - f'_2 = B$. At moment t_1 , the first radar works and after Δt , the first radar gets receiving signal. At moment t_2 , the second radar works. IF_1 is defined as the difference between transmitting signal 1 and receiving signal 2, and IF_2 is defined as the difference between transmitting signal 2 and receiving signal 1. Since $t_1 - t_2$ is much larger than Δt , IF_1 and IF_2 is much larger than Δf discussed

in section 2.1. Now we can move IF signal to larger frequency but we can still get Δf :

$$\Delta f = \frac{IF_1 - IF_2}{2} \quad (4.10)$$

Similarly, $f_1 - f'_1$ is much larger than Doppler shift generated by human walking. The equation of velocity information is still the same, but at least we can observe f_b^+ and f_b^- on the power spectrum.

In conclusion, the FMCW radar system shows the ability to position and track objects in short range. And my goal is to make the system more portable, economic and effective.

Appendix

Table 1 Range detection data

Distance (m)	Frequency (Hz)	Min Error (m)	Max Error (m)	Average Error (m)	SD (m)
0	0	0	0	0	0
0.45	600	0	0.0375	0.021428571	0.017359127
0.9	1200	0	0.0375	0.026785714	0.013258252
1.35	1800	0.01875	0.075	0.040178571	0.020044593
1.8	2400	0.01875	0.09375	0.050892857	0.022410536
2.25	3000	0.01875	0.09375	0.058928571	0.0254288
2.7	3600	0.0375	0.1125	0.066964286	0.024421316
3.15	4200	0.0375	0.13125	0.069642857	0.031693285
3.6	4800	0.05625	0.13125	0.080357143	0.027332587
4.05	5400	0.05625	0.1875	0.109821429	0.033240197
4.5	6000	0.05625	0.13125	0.123214286	0.03808143
4.95	6600	0.075	0.1875	0.128571429	0.034718254
5.4	7200	0.09375	0.24375	0.136607143	0.040633584
5.85	7800	0.075	0.1875	0.158035714	0.053033009
6.3	8400	0.09375	0.24375	0.16875	0.045927933
6.75	9000	0.075	0.24	0.173571429	0.050191597
7.2	9600	0.1125	0.24375	0.182142857	0.045653734
7.65	10200	0.13125	0.28125	0.211607143	0.051835721
8.05	10733.33333	0.13125	0.28125	0.219642857	0.052497608
8.5	11333.33333	0.13125	0.3	0.235714286	0.053445723
8.95	11933.33333	0.15	0.3	0.241071429	0.04674088
9.4	12533.33333	0.15	0.3375	0.265214286	0.057538147
9.85	13133.33333	0.16875	0.35625	0.283964286	0.062545805
10	13333.33333	0.16875	0.39375	0.308071429	0.072958885

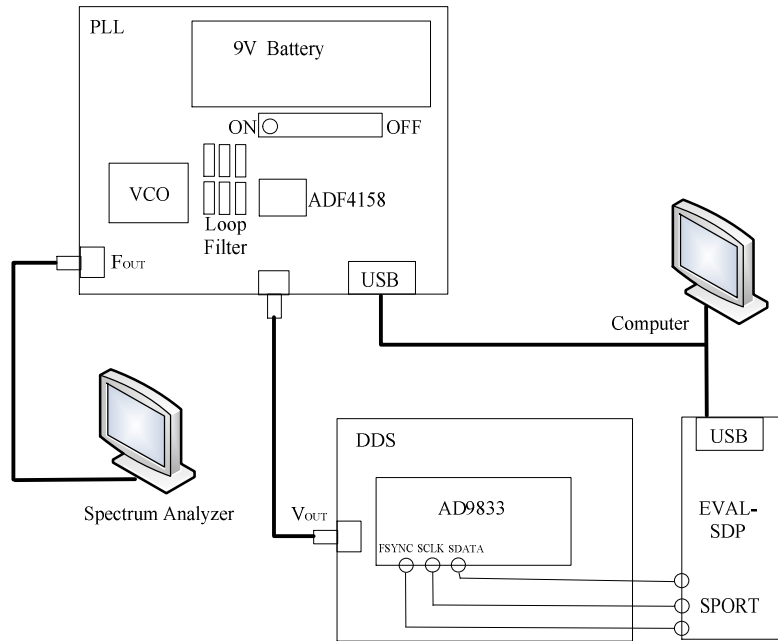


Figure 1 DDS-based PLL frequency synthesizer schematic

Table 2 DDS-based PLL Frequency Synthesizer Board Setups

Modes	Description
RF Setups	VCO output frequency=2.4 GHz Reference frequency=10 MHz R=1 N=240 Prescaler=4/5
Up Ramp	Frequency deviation per step = 40.016174 kHz Total ramp = 100 MHz Time per step = 0.2 us Time per ramp = 500 us
Down Ramp	Frequency deviation per step = 40.016174 kHz Total ramp = 100 MHz Time per step = 0.2 us Time per ramp = 500 us
PLL	R0=80780000 R1=1
Registers	R2=8012 R3=443 R4=180084 R5=11A0C85 R6=4E1E R7=7
DDS	f_{out} =12.5 MHz
Registers	Register=8000000

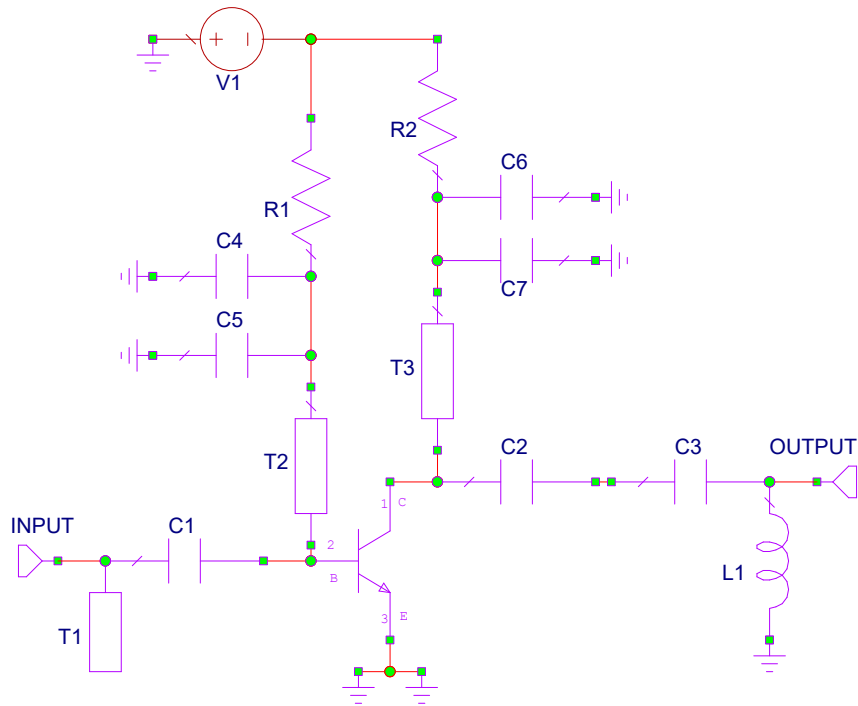


Figure 2 LNA schematic

Table 2 Bill of LNA Materials

Designator	Value	Description
T1	L=253.5 mil	Input Match
C1	15 pF	DC Blocking
C2	15 pF	DC Blocking
C3	1 pF	Output Match
L1	4.3 nH	Output Match
T2, T3	L=657.329 mil	LF Decoupling
C4, C6	1e5 pF	LF Decoupling
C5, C7	15 pF	LF Decoupling
R1	18.7 kOhm	Bias Network
R2	6 Ohm	Bias Network
V1	3.3 V	

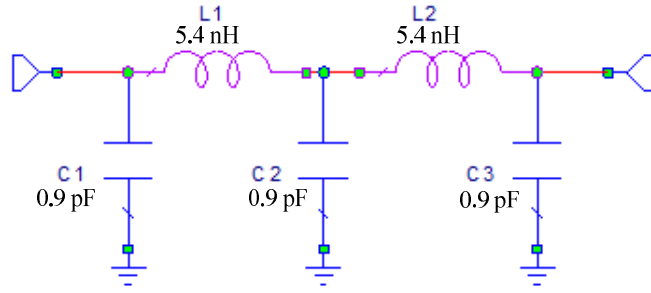


Figure 3 LPF schematic

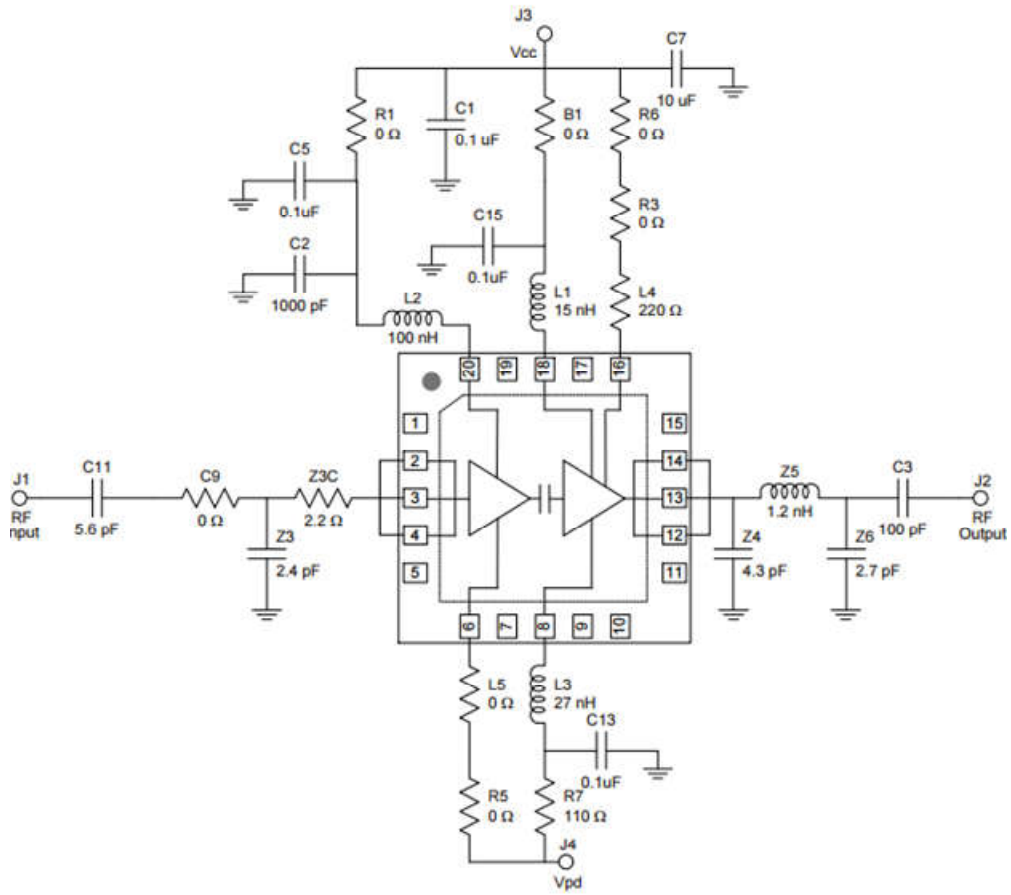


Figure 4 Power amplifier schematic

Bibliography

- [1] Mark A. Richards, “Fundamentals of Radar Signal Processing,” *McGraw-Hill Professional Company*, pp. 1-5, 2014.
- [2] Merrill I. Skolnik, “Introduction to Radar system,” *McGraw-Hill Professional Company*, pp. 1-14, 1981.
- [3] A.G. Stove, “Linear FMCW Radar Techniques,” *IEEE Proceedings-F*, Vol. 139, No. 5, pp. 825-830, 1992.
- [4] A.G. Stove, “Modern FMCW Radar – Techniques and Applications,” *European Radar Conference*, vol. 9, no.3, pp. 149-153, 2004.
- [5] Gitae Pyo, Choul-Young Kim and Songcheol Hong, “Single Antenna FMCW Radar CMOS Transceiver IC,” *IEEE Transactions on Microwave Theory and Techniques*, vol. 2, pp. 305-310, 2016.
- [6] Enxiao Liu, “The Receive and Transmit Front-end Design of X-band and Frequency Modulated Continuous Wave Radar”, *Dissertation Submitted to Hangzhou Dianzi University for the Degree of Master*, pp. 11-12, Dec, 2012.
- [7] Ronghui Zhang, “Transceiver Front-end for Short-range Target Detection”, *Dissertation Submitted to University of Electronic Science and Technology of China for the Degree of Master*, pp. 9-11, May, 2006.
- [8] Ahmed M. Eid, “System Simulation of RF Front-End Transceiver for Frequency Modulated Continuous Wave Radar”, *International Journal of Computer Application*, vol75, pp. 16-22, Aug. 2013.
- [9] Reza Sedaghati, “Analysis and Design of a Three-Phase PLL Structure”, *International Journal of Computer Science and Mobile Computing*, Vol.3 Issue.11, pp. 385-390, Nov, 2014.
- [10] Steven R. Richard, “CD4046B Types: CMOS Micropower Phase-Locked Loop,” *Texas Instruments*, Jul, 2003.
- [11] Ahmed M. Eid, “System Simulation of RF Front-End Transceiver for Frequency Modulated Continuous Wave Radar”, *International Journal of Computer Application*, vol75, pp. 16-22, Aug, 2013.
- [12] J. Schellenberg, R. Chedester and McCoy, “Multi-Channel Receiver for an E-band FMCW Imaging Radar”, *IEEE/MTT-S International Microwave Symposium*, pp. 1359-1362, 2013.

- [13] Eugin Hyun, Jong-Hun Lee, "A Method for Multi-target Range and Velocity Detection in Automotive FMCW Radar", *Proceedings of the 12th International IEEE Conference on Intelligent Transportation System*, PP. 7-11, 2009.
- [14] "Direct Modulation/Waveform Generating, 6.1 GHz Fractional-N Frequency Synthesizer", pp. 26-28, Feb, 2017.
- [15] A. Parssinen, J. Jussila, J. Ryyanen, L. Sumanen, K. Halonen, "A 2-GHz WideBand Direct Conversion Receiver for WCDMA Applications", *IEEE Journal of Solid-State Circuits*, vol 34, pp. 1893-1903, Dec, 1999.
- [16] Dennis Ma, "RF Receiver Systems and Circuits," pp. 2-13, 2014.
- [17] S. Wu, B. Razavi, "A 900-MHz/1.8-GHz CMOS Receiver for Dual-Band Applications", *IEEE Journal of Solid-State Circuits*, vol 33, pp. 2178-2185, Dec, 1998.
- [18] T. Liu, E. Westerwick, "5-GHz CMOS Radio Transceiver Front-End Chipset", *IEEE Journal of Solid-State Circuits*, vol 35, pp. 1927-1933, Dec, 2000.
- [19] B. Razavi, "RF Microelectronics", *Upper Saddle River*, pp. 153-158, 1998.
- [20] Govind Singh Patel, Sanjay Sharma, "Comparative Study of PLL, DDS and DDS-based PLL Synthesis Techniques for Communication System", *International Journal of Electronics Engineering*, pp. 35-40, 2010.
- [21] A. Bonfanti, F. Amorosa, C. Samori, and A. L. Lacaita, "A DDS-Based PLL for 2.4-GHz Frequency Synthesis", *IEEE Transactions on Circuits and Systems—ii: Analog and Digital Signal Processing*, vol. 50, no. 12, Dec, 2003.
- [22] B. G. Goldberg, "Digital Techniques in Frequency Synthesis", *McGraw-Hill*, 1986.
- [23] J. Jiang and E. K. F. Lee, "A ROM-less Direct Digital Frequency Synthesizer Using Segmented Nonlinear Digital-to-analog Converter", *2007 IEEE Region 10 Conference*, vol. 5, pp. 1272-1275, 2007.
- [24] Mickie P. Burt, "Range Correlation Effects in Radars", *IEEE Radar Conference*, Apr, 1993.
- [25] H. T. Nicholas III and H. Samueli, "An analysis of the output spectrum of direct digital frequency synthesizers in the presence of phase accumulator truncation", *Frequency Control Symp*, pp. 495–502, 1987.
- [26] Curtis Barrett, "Fractional/Integer-N PLL Basics", *Texas Instruments Application Note*, pp. 11-31, Aug, 1999.
- [27] Russia Pascal Nelson, "Design and Analysis Frequency Synthesizers Using FPGA as Reconfiguration Hardware", *Analog Devices Inc. (Greensboro, N.C.), EE Times*

Publication, pp. 45-48, Sep, 2003.

- [28] Govind Singh Patel¹, Sanjay Sharma, “Comparative Study of PLL, DDS and DDS-based PLL Synthesis Techniques”, *Communication System International Journal of Electronics Engineering*, vol2(1), pp. 35-40, 2010.
- [29] Saeed Golestan, Francisco D. Freijedo, Joseph M. Guerrero, “A Systematic Approach to Design Higher-Order Phase Locked Loops” *IEEE Trans. Power Electronics*, 2013.
- [30] S. Walters, T. Troudet, “Digital Phase-Locked Loop with Jitter Bounded”, *IEEE Transactions on Circuits and Systems*, 36, No. 7, pp. 189- 193, July 1989.
- [31] David Pozar, John Wiley, “Digital Techniques in Frequency Synthesis”, *McGraw-Hill Company*, 1986.
- [32] David Pozar, John Wiley, “Microwave Engineering”, *McGraw-Hill Company*, 2005.
- [33] Yong Wang, Yuanjin Zheng, “An FMCW Radar Transceiver Chip for Object Positioning and Human Limb Motion Detection”, *IEEE Sensors Journal*, VOL. 17, NO. 2, Jan, 2017.
- [34] Andreas Frischen, Jürgen Hasch and Christian Waldschmidt, “A Cooperative MIMO Radar Network Using Highly Integrated FMCW Radar Sensors”, *IEEE Transactions on Microwave Theory and Techniques*, VOL. 65, NO. 4, Apr, 2017.
- [35] Guochao Wang, Changzhan Gu, Takao Inoue and Changzhi Li, “A Hybrid FMCW-Interferometry Radar for Indoor Precise Positioning and Versatile Life Activity Monitoring”, *IEEE Transactions on Microwave Theory and Techniques*, VOL. 62, NO. 11, Nov, 2014.
- [36] A. Stelzer, M. Jahn and S. Scheiblhofer, “Radio and Wireless Symposium”, *2008 IEEE Radio and Wireless Symposium*, Mar, 2008.
- [37] Silvan Wehrli, David Barras, Frank Ellinger and Heinz Jackel, “Integrated Active Pulsed Reflector for FMCW Radar Localization”, *2009 IEEE MTT-S International Microwave Symposium Digest*, Jul, 2009.
- [38] Niko Joram, Belal Al-Qudsi, Jens Wagner, Axel Strobel and Frank Ellinger, “Design of a Multi-Band FMCW Radar Module”, *2013 10th Workshop on Positioning, Navigation and Communication (WPNC)*, Mar, 2013.